nature chemistry

SUPPLEMENTARY INFORMATION

https://doi.org/10.1038/s41557-019-0313-y

In the format provided by the authors and unedited.

A closed cycle for esterifying aromatic hydrocarbons with CO_2 and alcohol

Dianne J. Xiao[1], Emma D. Chant[1], Amy D. Frankhouser[1], Ying Chen[2], Allison Yau[1], Nancy M. Washton[2] and Matthew W. Kanan[1]*

[1]Department of Chemistry, Stanford University, Stanford, CA, USA. [2]Environmental Molecular Sciences Laboratory, Pacific Northwest National Laboratory, Richland, WA, USA. *e-mail: mkanan@stanford.edu

Supplementary Information

A Closed Cycle for Esterifying Aromatic Hydrocarbons with CO_2 and Alcohol

Dianne J. Xiao[1], Emma D. Chant[1], Amy D. Frankhouser[1], Ying Chen[2], Allison Yau[1], Nancy M. Washton[2], Matthew W. Kanan[1]

[1]*Department of Chemistry, Stanford University, Stanford, California, USA*
[2]*Environmental Molecular Sciences Laboratory, Pacific Northwest National Laboratory, Richland, Washington, USA*

Table of Contents **Page**

1. Methods

1.1 Materials

Anhydrous potassium carbonate (99.8%) was purchased from Fisher Chemical, cesium carbonate (99.99%) was purchased from Chem Impex International, titanium(IV) isopropoxide (≥98%) was purchased from Acros Organics, and methanol (99.9%, HPLC grade) was purchased from Fisher Chemical. Pellets of commercial TiO_2, ZrO_2, and γ-Al_2O_3 supports were purchased from Alfa Aesar and ground up in a mortar and pestle before use. Ordered mesoporous silica (SBA-15) was purchased from ACS Materials. ^{13}C-enriched potassium carbonate (98%), D_2O (99.9%) and benzene-d_6 (99.5%) were purchased from Cambridge Isotope Laboratories. Reagent-grade benzene was dried by passing through an activated alumina column on an Innovative Technology PureSolv solvent purification system, and then stored over 4 Å molecular sieves. CO_2 (99.5%) was purchased from Praxair. All other reagents were obtained from commercial vendors and used as received without further purification.

1.2. Synthesis of Cs_2CO_3/Mesoporous carbon

CMK-3 was prepared according to a previously reported procedure[1] with two additions of sucrose (1.30 g) in aqueous H_2SO_4 (0.3 M, 5.00 mL) to 1.00 g commercially purchased SBA-15 followed each time by drying (100 °C for 6 hours, 160 °C for 6 hours). Pyrolysis was done at 900 °C for 5 hours under N_2. The SBA-15 template was removed by stirring in 2 M KOH at 80 °C and the CMK-3 was washed with more 2 M KOH to ensure complete removal of the template. CMK-3 was then washed with water, methanol, and benzene and dried at 160 °C under flowing N_2. Washed CMK-3 was impregnated with a solution of Cs_2CO_3 in methanol (0.875 M, 0.800 mL/g) and dried under flowing N_2 (80°C, 0.5 h), followed by a second addition of 0.800 mL/g of the Cs_2CO_3/methanol solution. After thorough mixing with a spatula the material was dried under flowing N_2 (80 °C for 0.5 h, 160 °C for 1 h).

1.3. Characterization

Gas sorption measurements were collected on a Micromeritics ASAP 2020 instrument or a Quantachrome Autosorb iQ. Samples (~100 mg) were loaded into a preweighed tube, capped with a transeal, and then dried under vacuum (150 °C for at least 6 h). After drying, the evacuated tube was weighed again to determine the exact mass of the sample. Brunauer–Emmett–Teller (BET) surface areas, pore volumes, and pore size distributions were determined from N_2 adsorption/desorption isotherms collected at 77 K. The pore size distribution was calculated from the 77 K N_2 desorption data using the Barrett–Joyner–Halenda (BJH) method.

Scanning electron microscopy (SEM) samples of M_2CO_3/TiO_2 (0–3x) were prepared by drop casting powders suspended in ethyl acetate onto a silicon wafer. Samples were imaged at 5 kV using a FEI XL30 Sirion SEM with FEG source.

High-resolution synchrotron X-ray powder diffraction data for Cs_2CO_3/TiO_2 (1–3x) and K_2CO_3/TiO_2 (1–3x) were collected at Beamline 12.2.2 at the Advanced Light Source and Beamline 11-BM at the Advanced Photon Source, respectively. For pXRD data collection, all samples were dried under flowing N_2 (1 h, 150 °C) and vacuum (150 °C, 3 h) to remove residual water, and transferred to an N_2-filled glovebox. Borosilicate capillaries (1.0 mm diameter) were packed with sample inside the glovebox, sealed temporarily with silicone grease, and then immediately flame-sealed.

FT-IR spectra were collected on a Nicolet iS50 FT/IR Spectrometer in transmission mode using the KBr pellet method.

Scanning transmission electron microscopy (STEM) and energy dispersive spectroscopy (EDS) were performed on an FEI Tecnai G2 F20 X-TWIN Transmission Electron Microscope (TEM) equipped with an EDAX SUTW (super ultra thin window) detector and operated at 200 kV. EDS line scans were performed across the diameters of the particles with the EDS signal intensities recorded every 5 nm. TEM samples were prepared by drop casting ethyl acetate suspended powders onto 300 mesh Cu TEM grids from Ted Pella with 15-25 nm ultrathin carbon film on lacey carbon support film.

Solid state NMR spectra were collected on a Bruker spectrometer equipped with a 14.1 T magnet and operating at a ^{13}C carrier frequency of 150.93 MHz. $K_2{}^{13}CO_3/TiO_2$ (1–3x) samples were prepared according to the method described above using ^{13}C-enriched starting material. For room temperature experiments, $K_2{}^{13}CO_3/TiO_2$ or bulk $K_2{}^{13}CO_3$ was loaded into a standard 5 mm rotor. Samples examined at elevated temperature were prepared using 5 mm "WHiMS" rotors, described in detail elsewhere[2], which were sealed under ambient conditions using Vespel fittings and Kel-F o-rings. Spectra were collected with 5 kHz MAS in a custom high temperature 5 mm HX probe.

^{13}C direct polarization spectra were averaged from either 32 scans collected with 90 degree pulse width and a relaxation delay of 1000 s, or 128 scans collected with a 30 degree pulse width and a relaxation delay of 200 s. Sample heating up to 320 °C was achieved by heating of both variable temperature (VT) and bearing gas inlets to minimize temperature gradient across the sample[3]. The sample temperature was calibrated by measuring changes in the ^{207}Pb resonance of solid $Pb(NO_3)_2$[4]. ^{13}C peak areas were quantified with deconvolution using the "sola" solid state peak-fitting program as implemented in Bruker TopSpin software. T_1 relaxation was quantified via inversion recovery.

Surface titration experiments were performed according to a modified version of a previously reported procedure[5,6] using M_2CO_3/TiO_2 samples that had been dried at 150 °C under vacuum for at least 4 h to remove residual H_2O. In an inert atmosphere glovebox, various quantities of 4-nitrophenol (0.2 wt% in benzene, pK_a = 7.2 in H_2O) were added to M_2CO_3/TiO_2 (50 mg in 2 mL benzene), causing the sample to turn yellow as surface carbonates deprotonate the phenolic proton. The sample was equilibrated for ~15 minutes with periodic gentle shaking, after which phenolphthalein (saturated solution in benzene, 2 mL) was added. The sample was equilibrated overnight. If the amount of 4-nitrophenol was insufficient to quench all the surface carbonates, the sample darkened and gained a red/violet hue due to the presence of deprotonated phenolphthalein. Note that benzoic acid (pK_a = 4.2 in H_2O) and other acids that might be strong enough to protonate HCO_3^- were avoided, in order to prevent H_2O formation and dissolution of surface alkali salts.

1.4. Product analysis

^{1}H-NMR and ^{13}C-NMR spectra were recorded at 23 °C on a Varian Unity Inova 500 MHz spectrometer, Varian Direct Drive 400 MHz spectrometer, Varian Mercury 400 MHz spectrometer, or Varian Unity Inova 300 MHz spectrometer. ^{1}H chemical shifts (δ) are reported in parts per million (ppm) downfield from tetramethylsilane and referenced to residual protium in the NMR solvent (D_2O, δ = 4.79, CDCl3, δ = 7.26). ^{13}C chemical shifts (δ) are reported in parts per million downfield from tetramethylsilane and referenced to carbon resonances in the NMR solvent ($CDCl_3$ δ = 77.16, center line), or to added methanol (δ = 49.50 in D_2O).

For biphenyl and naphthalene substrates, reactions were also separately analyzed by HPLC using an Agilent 1200 HPLC equipped with a diode array detector and an Agilent Eclipse XDB-C18 reverse phase column. The HPLC samples were prepared by diluting and neutralizing an aliquot of the D_2O NMR sample with CH_3CN containing 0.1% trifluoroacetic acid (TFA). Biphenyl carboxylation analyses were carried out at 40 °C with 70% H_2O and 30% CH_3CN (0.1% TFA) as the mobile phase at a total flow rate of 1.5 mL/min. Naphthalene carboxylation analyses were carried out at 40 °C using a gradient method, beginning with 80% H_2O and 20% CH_3CN (0.1% TFA), and ending with 70% H_2O and 30% CH_3CN (0.1% TFA) as the mobile phase. For DMC methylation analysis, the HPLC samples were prepared by diluting an aliquot of the contents of the cold trap. DMC methylation analyses were carried out at room temperature with 70% H_2O and 30% CH_3CN as the mobile phase. Calibration curves were constructed using solutions of pure compounds at known concentrations.

Mass spectrometry was performed on an HP 7890/5975 GC-MS, a single quadrupole MS with an electron impact ionization source.

1.5. Mechanistic studies

For H/D exchange experiments, a 27.5 mL stainless steel reactor was loaded with 20 μL of 1:1 C_6H_6:C_6D_6, and either M_2CO_3/TiO_2 (333 mg) or bulk M_2CO_3 (500 mg). The reactor was sealed, attached to a gas-dosing manifold, degassed by freeze-pump-thawing, and pressurized with N_2 (1 bar at room temperature). The reactor was heated to 400 °C for 12 h. After cooling, the benzene was extracted from the reaction vessel using Et_2O (10 mL) and analyzed by GC-MS.

Kinetic isotope effects were measured via competition experiments using mixtures of C_6H_6 and C_6D_6 (1:1, 1:2, and 1:4). Typical benzene carboxylation experiment procedures were followed. The reaction was run at 380 °C for 0.5 h to prevent product scrambling. Following carboxylation, the alkali salts were extracted from the support (3 x 10 mL H_2O, 70 °C) and dried to a solid. The carboxylates were esterified using H_2SO_4/MeOH (60 °C, overnight). An aliquot of this solution was neutralized using excess solid K_2CO_3, diluted in Et_2O, filtered, and analyzed by GC-MS.

1.6. NMR References

NMR peaks were assigned to the different products by comparison to spectra from pure compounds, or Cs^+ salts obtained independently from the pure carboxylic acids. The resonances for these compounds are provided below for reference. (Note: Depending on the salt/base concentration of the D_2O sample, the ^1H peaks may shift slightly compared to these references.)

Cesium benzoate
^{1}H-NMR (500 MHz, D_2O) δ 7.80 (d, *J* = 7.5 Hz, 2H), 7.41 (t, *J* = 7.5 Hz, 1H), 7.36 (t, *J* = 7.5 Hz, 2H)
^{13}C-NMR (125MHz, D_2O) δ 176.0, 137.0, 131.9, 129.5, 129.0

Cesium 1,2-benzenedicarboxylate (cesium phthalate)
^{1}H-NMR (500 MHz, D_2O) δ 7.45 (dd, *J* = 5.7, 3.3 Hz, 2H), 7.37 (dd, *J* = 5.7, 3.3 Hz, 2H)
^{13}C-NMR (125MHz, D_2O) δ 177.8, 138.5, 129.5, 127.8

Cesium 1,3-benzenedicarboxylate (cesium isophthalate)
^{1}H-NMR (500 MHz, D_2O) δ 8.25 (S, 1H), 7.89 (d, *J* = 7.7 Hz, 2H), 7.39 (t, *J* = 7.7 Hz, 1H)
^{13}C-NMR (125MHz, D_2O) δ 175.5, 137.1, 132.1, 129.7, 129.0

Cesium 1,4-benzenedicarboxylate (cesium terephthalate)
^{1}H-NMR (500MHz, D_2O) δ 7.80 (s, 4H)
^{13}C-NMR (125MHz, D_2O) δ 175.5, 139.4, 129.3

Cesium biphenyl-2-carboxylate
^{1}H-NMR (500MHz, D_2O) δ 7.49 – 7.35 (m, 9H)
^{13}C-NMR (125MHz, D_2O) δ 179.4, 141.9, 140.1, 138.8, 130.4, 129.4, 129.3, 129.0, 128.1, 128.0, 127.5

Cesium biphenyl-3-carboxylate
^{1}H-NMR (500MHz, D_2O) δ 8.10 (s, 1H), 7.83 (d, *J* = 7.7 Hz, 1H), 7.76 (d, *J* = 7.7 Hz, 1H), 7.72 – 7.66 (m, 2H), 7.55 – 7.46 (m, 3H), 7.41 (t, *J* = 7.5 Hz, 1H).
^{13}C-NMR (125MHz, D_2O) δ 175.5, 140.8, 140.5, 137.6, 129.9, 129.5, 129.4, 128.5, 128.1, 127.9, 127.3.

Cesium biphenyl-4-carboxylate
^{1}H-NMR (500MHz, D_2O) δ 7.91 (d, *J* = 8.6, 2H), 7.72 – 7.66 (m, 4H), 7.53 – 7.45 (m, 2H), 7.42 (t, *J* = 7.4 Hz, 1H).
^{13}C-NMR (125MHz, D_2O) δ 175.8, 143.6, 140.3, 135.8, 130.2, 129.7, 128.6, 127.6, 127.2.

Cesium 1-naphthoate
^{1}H-NMR (500MHz, D_2O) δ 8.15 (d, *J* = 8.2 Hz, 1H), 7.92 (d, *J* = 7.7 Hz, 1H), 7.90 (d, *J* = 7.7 Hz, 1H), 7.58 – 7.47 (m, 4H).
^{13}C-NMR (125MHz, D_2O) δ 178.52, 138.39, 134.00, 129.92, 129.57, 128.94, 127.37, 126.86, 126.37, 126.08, 125.05.

Cesium 2-naphthoate
^{1}H-NMR (400 MHz, D_2O) δ 8.33 (s, 1H), 7.95 (d, *J* = 7.5 Hz, 1H), 7.90 – 7.85 (m, 3H), 7.57 – 7.50 (m, 2 H).
^{13}C-NMR (125 MHz, D_2O) δ 175.94, 134.81, 134.29, 132.94, 129.84, 129.46, 128.26, 128.02, 127.99, 127.01, 126.29.

Cesium acetate
^{1}H-NMR (400MHz, D_2O) δ 1.87 (s, 3H)
^{13}C-NMR (100MHz, D_2O) δ 181.4, 23.6

Cesium formate
^{1}H-NMR (400MHz, D_2O) δ 8.45 (s, 1H)
^{13}C-NMR (100MHz, D_2O) δ 171.12

Methyl benzoate
^{1}H-NMR (500MHz, $CDCl_3$) δ 8.03 (d, *J* = 8.4 Hz, 2H), 7.52 (t, *J* = 7.5 Hz, 1H), 7.44–7.37 (m, 2H), 3.88 (s, 3H)
^{13}C-NMR (125MHz, $CDCl_3$) δ 167.1, 132.9, 130.2, 129.6, 128.4, 52.0

2. Supplementary Tables

Supplementary Table 1 | Surface areas, pore volumes, and pore diameters of K_2CO_3 and Cs_2CO_3/TiO_2 at various loadings, calculated from 77 K N_2 adsorption/desorption isotherms. 1x = 0.56 mmol M_2CO_3/g TiO_2; 2x = 1.12 mmol M_2CO_3/g TiO_2; 3x = 1.68 mmol M_2CO_3/g TiO_2. (Note that Cs_2CO_3 samples show greater reductions in surface area and pore volume at every given loading due to its heavier molecular weight.)

Sample	**BET Surface Area** (m^2/g)	**Pore volume** (cm^3/g)	**Pore diameter**[1] (nm)
TiO_2 (0x)	112.2(5)	0.32	10.7
K_2CO_3/TiO_2 (1x)	90.7(2)	0.27	10.9
K_2CO_3/TiO_2 (2x)	72.6(2)	0.22	10.7
K_2CO_3/TiO_2 (3x)	65.4(2)	0.19	9.2
Cs_2CO_3/TiO_2 (1x)	76.6(2)	0.24	11.0
Cs_2CO_3/TiO_2 (2x)	51.7(2)	0.19	11.1
Cs_2CO_3/TiO_2 (3x)	36.5(2)	0.13	11.2

[1]The maximum of the pore size distribution plot, which was calculated by the Barrett–Joyner–Halenda (BJH) method from 77 K N_2 isotherm data (desorption branch).

Supplementary Table 2 | Surface areas, pore volumes, and pore diameters of Cs_2CO_3/TiO_2 (1x) and K_2CO_3/TiO_2 (1x) before and after 10x benzene CO_2 insertion cycling experiments, calculated from 77 K N_2 adsorption/desorption isotherms. Larger changes in surface area and pore diameter were observed in K_2CO_3 relative to Cs_2CO_3/TiO_2 (1x) because the carboxylation reactions were performed for significantly longer times (3 h at 440 °C versus 0.5 h at 440 °C), leading to greater sintering of the TiO_2 support.

Sample	**BET Surface Area** (m^2/g)	**Pore volume** (cm^3/g)	**Pore diameter**[1] (nm)
K_2CO_3/TiO_2 (1x)	90.7(2)	0.27	10.9
K_2CO_3/TiO_2 (1x), post 10x cycles	73.0(3)	0.26	13.6
Cs_2CO_3/TiO_2 (1x)	76.6(2)	0.24	11.0
Cs_2CO_3/TiO_2 (1x), post 10x cycles	77.7(3)	0.25	10.9

[1]The maximum of the pore size distribution plot, which was calculated by the Barrett–Joyner–Halenda (BJH) method from 77 K N_2 isotherm data (desorption branch).

Supplementary Table 3 | Surface areas, pore volumes, and pore diameters of Cs_2CO_3 loaded onto a commercial TiO_2 support, calculated from 77 K N_2 adsorption/desorption isotherms. Carbonate loadings were 0.30 mmol/g TiO_2.

Sample	**BET Surface Area** (m^2/g)	**Pore volume** (cm^3/g)	**Pore diameter**[1] (nm)
TiO_2 (commercial, 0x)	38.1(4)	0.17	11.3
Cs_2CO_3/TiO_2 (commercial, 1x)	28.4(1)	0.15	11.2

[1]The maximum of the pore size distribution plot, which was calculated by the Barrett–Joyner–Halenda (BJH) method from 77 K N_2 isotherm data (desorption branch).

Supplementary Table 4 | Summary of benzene carboxylation yields for K_2CO_3/TiO_2 (1x) as a function of temperature. Yields were determined by aqueous extraction of the carboxylates from the support followed by ^1H NMR analysis. K_2CO_3/TiO_2 (1x) is loaded with 0.56 mmol M_2CO_3/g TiO_2; 100% CO_3^{2-} conversion corresponds to 2 equivalents of carboxylate formation. Conditions: 20 bar benzene, 10 bar CO_2, 3 h reaction time.

Sample	**T** (°C)	**Benzoate** (μmol/g TiO_2)	**Di-carboxylates**[1] (μmol/g TiO_2)	**Benzoate selectivity** (%)	**CO_3^{2-} converted** (%)
K_2CO_3/TiO_2 (1x; 0.56 mmol CO_3^{2-}/g TiO_2)	400	25	2	91	3
K_2CO_3/TiO_2 (1x)	420	70	10	88	8
K_2CO_3/TiO_2 (1x)	440	99	10	90	11

[1]Trace acetate, formate, and tricarboxylates (<1 μmol/g TiO_2) were also observed.

Supplementary Table 5 | Summary of benzene carboxylation yields for Cs_2CO_3/TiO_2 (1x) as a function of temperature. Yields were determined by aqueous extraction of the carboxylates from the support followed by ^1H NMR analysis. Cs_2CO_3/TiO_2 (1x) is loaded with 0.56 mmol M_2CO_3/g TiO_2; 100% CO_3^{2-} conversion corresponds to 2 equivalents of carboxylate formation. Conditions: 20 bar benzene, 10 bar CO_2, 3 h reaction time.

Sample	**T** (°C)	**Benzoate** (μmol/g TiO_2)	**Di-carboxylates**[1] (μmol/g TiO_2)	**Benzoate selectivity** (%)	**CO_3^{2-} converted** (%)
Cs_2CO_3/TiO_2 (1x)	380	37	*trace*	96	4
Cs_2CO_3/TiO_2 (1x)	400	56	5	92	6
Cs_2CO_3/TiO_2 (1x)	420	92	13	88	11
Cs_2CO_3/TiO_2 (1x)	440[2]	78	10	89	9

[1]Trace acetate, formate, and tricarboxylates (<1 μmol/g TiO_2) were also observed.
[2]Reaction was performed for 0.5 h.

Supplementary Table 6 | Summary of benzene carboxylation yields for Cs_2CO_3 dispersed on a commercial TiO_2 support. Yields were determined by aqueous extraction of the carboxylates from the support followed by ^1H NMR analysis. Cs_2CO_3/TiO_2 (commercial, 1x) is loaded with 0.30 mmol M_2CO_3/g TiO_2; 100% CO_3^{2-} conversion corresponds to 2 equivalents of carboxylate formation. Conditions: 20 bar benzene, 10 bar CO_2, 3 h reaction time.

Sample	**T** (°C)	**Benzoate** (μmol/g TiO_2)	**Di-carboxylates**[1] (μmol/g TiO_2)	**Benzoate selectivity** (%)	**CO_3^{2-} converted** (%)
Cs_2CO_3/TiO_2 (commercial, 1x)	380	18	*trace*	95	3
Cs_2CO_3/TiO_2 (commercial, 1x)	400	40	5	89	8
Cs_2CO_3/TiO_2 (commercial, 1x)	420	53	9	85	12
Cs_2CO_3/TiO_2 (commercial, 1x)	440	51	9	84	12

[1]Trace acetate, formate, and tricarboxylates (<1 μmol/g TiO_2) were also observed.

Supplementary Table 7 | Summary of benzene carboxylation yields for K_2CO_3/TiO_2 and Cs_2CO_3/TiO_2 as a function of loading (1–3x), where the carbonate loadings are 1x = 0.56, 2x = 1.12, and 3x = 1.68 mmol M_2CO_3/g TiO_2. Yields were determined by aqueous extraction of the carboxylates from the support followed by ^{1}H NMR analysis. 100% CO_3^{2-} conversion corresponds to 2 equivalents of carboxylate formation. Conditions: 20 bar benzene, 10 bar CO_2, 3 h reaction time.

Sample	**T** (°C)	**Benzoate** (μmol/g TiO_2)	**Di-carboxylates**[1] (μmol/g TiO_2)	**Benzoate selectivity** (%)	**CO_3^{2-} converted** (%)
K_2CO_3/TiO_2 (1x)	420	70	10	88	8
K_2CO_3/TiO_2 (2x)	420	62	10	86	4
K_2CO_3/TiO_2 (3x)	420	50	11	81	2
Cs_2CO_3/TiO_2 (1x)	420	92	13	88	11
Cs_2CO_3/TiO_2 (2x)	420	86	15	85	5
Cs_2CO_3/TiO_2 (3x)	420	82	30	72	4

[1]Trace acetate, formate, and tricarboxylates (<1 μmol/g TiO_2) were also observed.

Supplementary Table 8 | Summary of benzene carboxylation yields for Na_2CO_3/TiO_2 and MgO nanoparticles (<50 nm). Yields were determined by aqueous extraction of the carboxylates from the support followed by ^1H NMR analysis. Na_2CO_3/TiO_2 (1x) is loaded with 0.56 mmol Na_2CO_3/g TiO_2; 100% CO_3^{2-} conversion corresponds to 2 equivalents of carboxylate formation. For MgO, excess K_2CO_3 was added during the extraction procedure to aid removal of any surface carboxylates. Conditions: 20 bar benzene, 10 bar CO_2, 3 h reaction time.

Sample	**T** (°C)	**Benzoate** (μmol/g TiO_2)	**Di-carboxylates** (μmol/g TiO_2)	**Benzoate selectivity** (%)	**CO_3^{2-} converted** (%)
Na_2CO_3/TiO_2 (1x)	420	17	*trace*	95	1.7
Na_2CO_3/TiO_2 (1x)	440	31	*trace*	93	3
MgO	420	1[1]	*trace*	N/A	N/A
MgO	440	2[1]	*trace*	N/A	N/A

[1] μmol/g MgO

Supplementary Table 9 | Summary of biphenyl carboxylation yields for Cs_2CO_3/TiO_2 (1x). Yields were determined by aqueous extraction of the carboxylates from the support followed by ^1H NMR and HPLC analysis. Cs_2CO_3/TiO_2 (1x) is loaded with 0.56 mmol M_2CO_3/g TiO_2; 100% CO_3^{2-} conversion corresponds to 2 equivalents of carboxylate formation. Conditions: 600 mg biphenyl (7 to 8 bar, depending on reaction temperature), 10 bar CO_2, 3 h reaction time.

Sample	**T** (°C)	**2-BP-carboxylate** (μmol/g TiO_2)	**3-BP-carboxylate** (μmol/g TiO_2)	**4-BP-carboxylate** (μmol/g TiO_2)	**Di-carboxylates**[1] (μmol/g TiO_2)	**CO_3^{2-} converted** (%)
Cs_2CO_3/TiO_2 (1x)	380	7	19	11	*trace*	4
Cs_2CO_3/TiO_2 (1x)	400	7	46	29	17	10
Cs_2CO_3/TiO_2 (1x)	420	4	63	42	20	13
Cs_2CO_3/TiO_2 (1x)	440[2]	7	53	32	14	11

[1]Trace acetate, formate, and tricarboxylates (<1 μmol/g TiO_2) were also observed.
[2]Reaction was performed for 0.5 h.

Supplementary Table 10 | Summary of naphthalene carboxylation yields for Cs_2CO_3/TiO_2 (1x), as well as Cs_2CO_3 supported on a commercial TiO_2 support. Yields were determined by aqueous extraction of the carboxylates from the support followed by ^1H NMR and HPLC analysis. Cs_2CO_3/TiO_2 (1x) is loaded with 0.56 mmol M_2CO_3/g TiO_2; Cs_2CO_3/TiO_2 (commercial, 1x) is loaded with 0.30 mmol M_2CO_3/g TiO_2; 100% CO_3^{2-} conversion corresponds to 2 equivalents of carboxylate formation. Conditions: 250 mg naphthalene (~4 bar), 10 bar CO_2, 3 h reaction time.

Sample	**T** (°C)	**2-naphthoate** (μmol/g TiO_2)	**1-naphthoate** (μmol/g TiO_2)	**Di-carboxylates** (μmol/g TiO_2)	**CO_3^{2-} converted** (%)
Cs_2CO_3/TiO_2 (commercial, 1x)	380	21.5	7.3	3.4	6
Cs_2CO_3/TiO_2 (commercial, 1x)	400	30.9	13.6	6.9	10
Cs_2CO_3/TiO_2 (commercial, 1x)	420	32.3	6.6	5.9	9
Cs_2CO_3/TiO_2 (commercial, 1x)	440	32.3	7.9	4.5	8
Cs_2CO_3/TiO_2 (1x)	400	55.9	9.7	14.5	8

Supplementary Table 11 | Surface areas, pore volumes, and pore diameters of several commercial mesoporous supports (ZrO_2, γ-Al_2O_3, and ordered mesoporous carbon) loaded with M_2CO_3, calculated from 77 K N_2 adsorption/desorption isotherms. Optimal carbonate loadings vary based on the support surface area and pore volume, and were empirically determined based on reactivity studies.

Sample	**BET Surface Area** (m^2/g)	**Pore volume** (cm^3/g)	**Pore diameter**[1] (nm)
ZrO_2	98.3(4)	0.30	7.7
Cs_2CO_3/ZrO_2 (**0.53 mmol/g** ZrO_2)	66.9(3)	0.22	7.1
γ-Al_2O_3	251.1(11)	0.83	8.2
Cs_2CO_3/γ-Al_2O_3 (**1.45 mmol/g** γ-Al_2O_3)	122.8(5)	0.43	7.5
Ordered mesoporous carbon (CMK-3)	1062.8(37)	0.90	4.2
Cs_2CO_3/CMK-3 (**1.40 mmol/g** CMK-3)	497.7(20)	0.51	4.2

[1]The maximum of the pore size distribution plot, which was calculated by the Barrett–Joyner–Halenda (BJH) method from 77 K N_2 isotherm data (desorption branch).

Supplementary Table 12 | Summary of benzene carboxylation yields for Cs_2CO_3 loaded onto different mesoporous support materials (TiO_2, ZrO_2, γ-Al_2O_3, and ordered mesoporous carbon). Optimal carbonate loadings varied based on the support surface chemistry and surface area, and were empirically determined based on reactivity studies. Yields were determined by aqueous extraction of the carboxylates from the support followed by ^{1}H NMR analysis. 100% CO_3^{2-} conversion corresponds to 2 equivalents of carboxylate formation. Conditions: 20 bar benzene, 10 bar CO_2, 420 °C, 3 h reaction time.

Sample	**Total carboxylates**[1] (μmol/g support)	**Total carboxylates**[1] (μmol/g M_2CO_3/support)	**Benzoate selectivity** (%)	**CO_3^{2-} converted** (%)
Cs_2CO_3/TiO_2 (**0.56 mmol/g** TiO_2)	104	88	88	11
Cs_2CO_3/ZrO_2 (**0.53 mmol/g** ZrO_2)	121	103	85	13
Cs_2CO_3/γ-Al_2O_3 (**1.45 mmol/g** γ-Al_2O_3)	244	164	87	10
Cs_2CO_3/carbon (**1.40 mmol/g** carbon)	522	359	60	26

[1]Sum of mono and di-carboxylates formed in the reaction.

Supplementary Table 13 | Summary of the influence of dimethyl carbonate (DMC) on benzoate methylation yields. Surface-bound benzoates in carboxylated $Cs_2CO_3/\gamma\text{-}Al_2O_3$ and K_2CO_3/carbon were exposed to a) flowing mixtures of MeOH and CO_2, or b) flowing mixtures of DMC and N_2. The volatilized methyl benzoate was trapped in a downstream cold trap. Methyl benzoate was quantified by HPLC analysis of the trapped material, or by hydrolysis of the trapped material followed by ^{1}H NMR analysis. Yields are given with respect to the amount of benzoate formed in the carboxylation reaction (Supplementary Table 12). Methylation conditions under flowing MeOH/CO_2: 1.8 bar MeOH, 1.2 bar CO_2, flowing 100 ml/min at 280 °C for 2 h. Methylation conditions under flowing DMC/N_2: 0.3 bar DMC, 0.7 bar N_2 for $\gamma\text{-}Al_2O_3$ and 2.7 bar N_2 for carbon, flowing 50 mL/min at 250 °C for 1 h.

Sample	**Methylation conditions**	**Methyl benzoate yield** (%)
Cs_2CO_3/ZrO_2 (**0.53 mmol/g** ZrO_2)	MeOH/CO_2	36
$Cs_2CO_3/\gamma\text{-}Al_2O_3$ (**1.45 mmol/g** $\gamma\text{-}Al_2O_3$)	MeOH/CO_2	7
$Cs_2CO_3/\gamma\text{-}Al_2O_3$ (**1.45 mmol/g** $\gamma\text{-}Al_2O_3$)	DMC/N_2	88
Cs_2CO_3/carbon (**1.40 mmol/g** carbon)	MeOH/CO_2	*trace*
Cs_2CO_3/carbon (**1.40 mmol/g** carbon)	DMC/N_2	75[1]

[1]Trace amounts of dicarboxylates were observed in the cold trap after methylation with DMC.

Supplementary Table 14 | Amount of dicarboxylates remaining on Cs_2CO_3/TiO_2 (1x) and K_2CO_3/TiO_2 (1x) after one cycle, ten cycles, and after heating at 440 °C under N_2 for 3 h. Yields were determined by aqueous extraction of the dicarboxylates from the support followed by ^1H NMR analysis. Cs_2CO_3 and K_2CO_3/TiO2 (1x) are loaded with 0.56 mmol M_2CO_3/g TiO_2; 100% CO_3^{2-} conversion corresponds to 2 equivalents of carboxylate formation. Carboxylation conditions: 20 bar benzene, 10 bar CO_2, 440 °C, for either 0.5 h (Cs_2CO_3) or 3 h (K_2CO_3) reaction time. Methylation conditions: 1.8 bar MeOH, 1.2 bar CO_2, flowing 100 ml/min for 1 h at either 250 °C (Cs_2CO_3) or 280 °C (K_2CO_3).

Sample	**Di-carboxylates recovered on support** (μmol/g TiO_2)	**Tri-carboxylates recovered on support** (μmol/g TiO_2)
Cs_2CO_3/TiO_2 (1x), after 1x cycle	10	–
Cs_2CO_3/TiO_2 (1x), after 10x cycles	21	–
Cs_2CO_3/TiO_2 (1x), after 1x cycle and 440 °C in N_2	2	–
Ks_2CO_3/TiO_2 (1x), after 1x cycle	10	–
K_2CO_3/TiO_2 (1x), after 10x cycles	6	–
K_2CO_3/TiO_2 (1x), after 1x cycle and 440 °C in N_2	6	–

3. Supplementary Figures

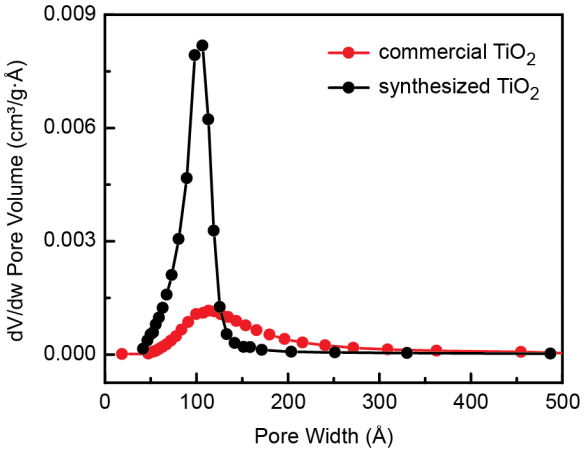

Supplementary Figure 1 | Pore size distribution plots of commercial and synthesized bare TiO_2 samples, calculated using the Barrett–Joyner–Halenda (BJH) method from 77 K N_2 isotherm data (desorption branch).

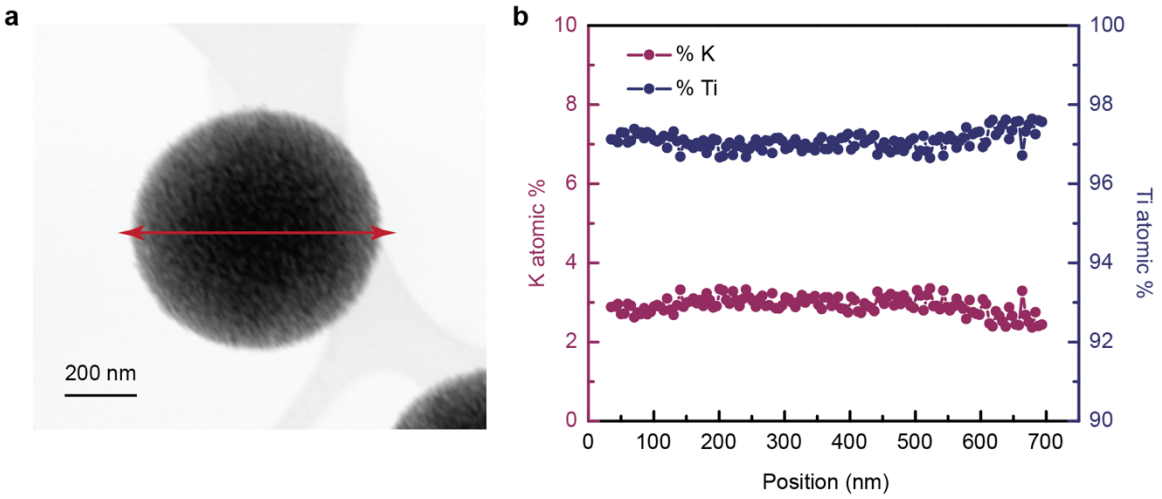

Supplementary Figure 2 | STEM EDS elemental analysis data for K_2CO_3/TiO_2 (1x) showing K_2CO_3 is homogeneously dispersed within a particle. **a**, STEM bright field image of a K_2CO_3/TiO_2 particle. A line scan was performed across the diameter of the particle as shown, with EDS spectra taken every ~5 nm. **b**, Relative atomic percentages of K and Ti across the diameter of a single particle of K_2CO_3/TiO_2 (1x), calculated from EDS data. Our experimentally determined percentages (~3% K, 97% Ti) are lower than the theoretically calculated percentages (8% K, 92% Ti). However, analysis of eight different particles gave a consistent %K value of 3.3(7) %. Therefore, differences between experimental/theoretical values are likely because of a systematic error in the EDS calibration for K, and not because of inhomogeneous loading.

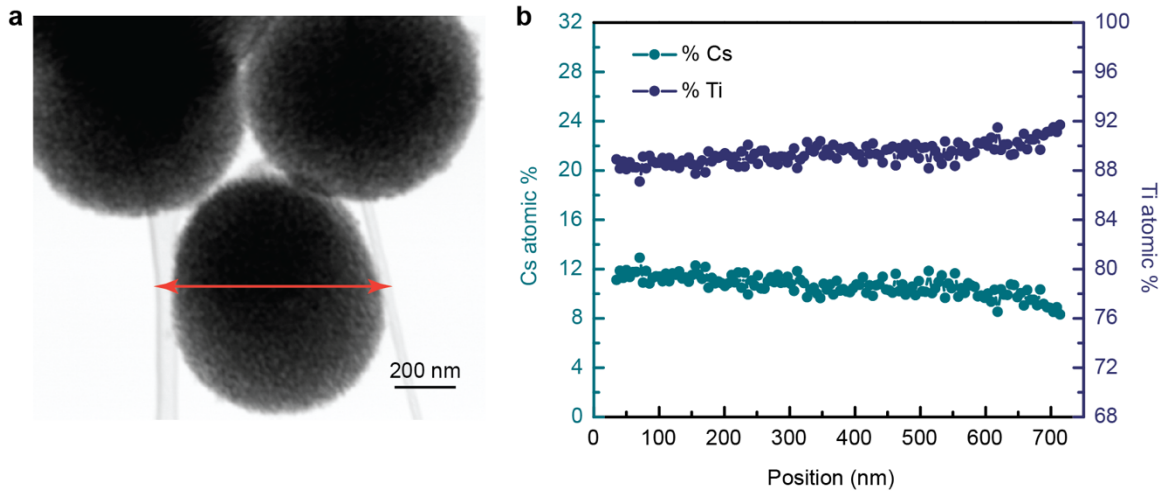

Supplementary Figure 3 | STEM EDS elemental analysis data for Cs_2CO_3/TiO_2 (1x) showing Cs_2CO_3 is homogeneously dispersed within a particle. **a**, STEM bright field image of a Cs_2CO_3/TiO_2 particle. A line scan was performed across the diameter of the particle as shown, with EDS spectra taken every ~5 nm. **b**, Relative atomic percentages of Cs and Ti across the diameter of a single particle of Cs_2CO_3/TiO_2 (1x), calculated from EDS data. Our experimentally determined percentages (~11% Cs, 89% Ti) are within error of the theoretical percentages at this loading (8% Cs, 92% Ti).

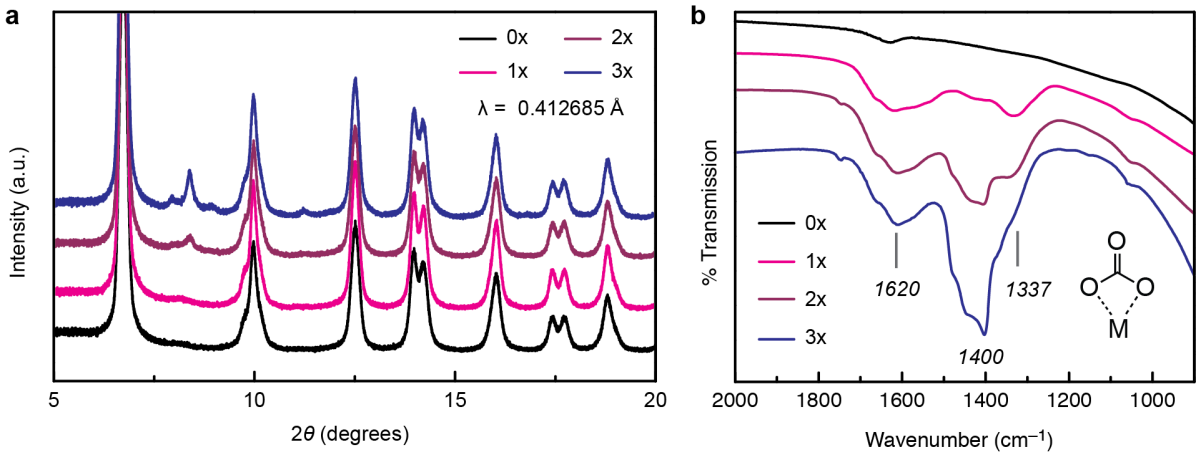

Supplementary Figure 4 | **a**, pXRD patterns (λ = 0.412685 Å) of K_2CO_3/TiO_2 as a function of loading (1–3x). **b**, IR spectra of K_2CO_3/TiO_2 as a function of loading (1–3x).

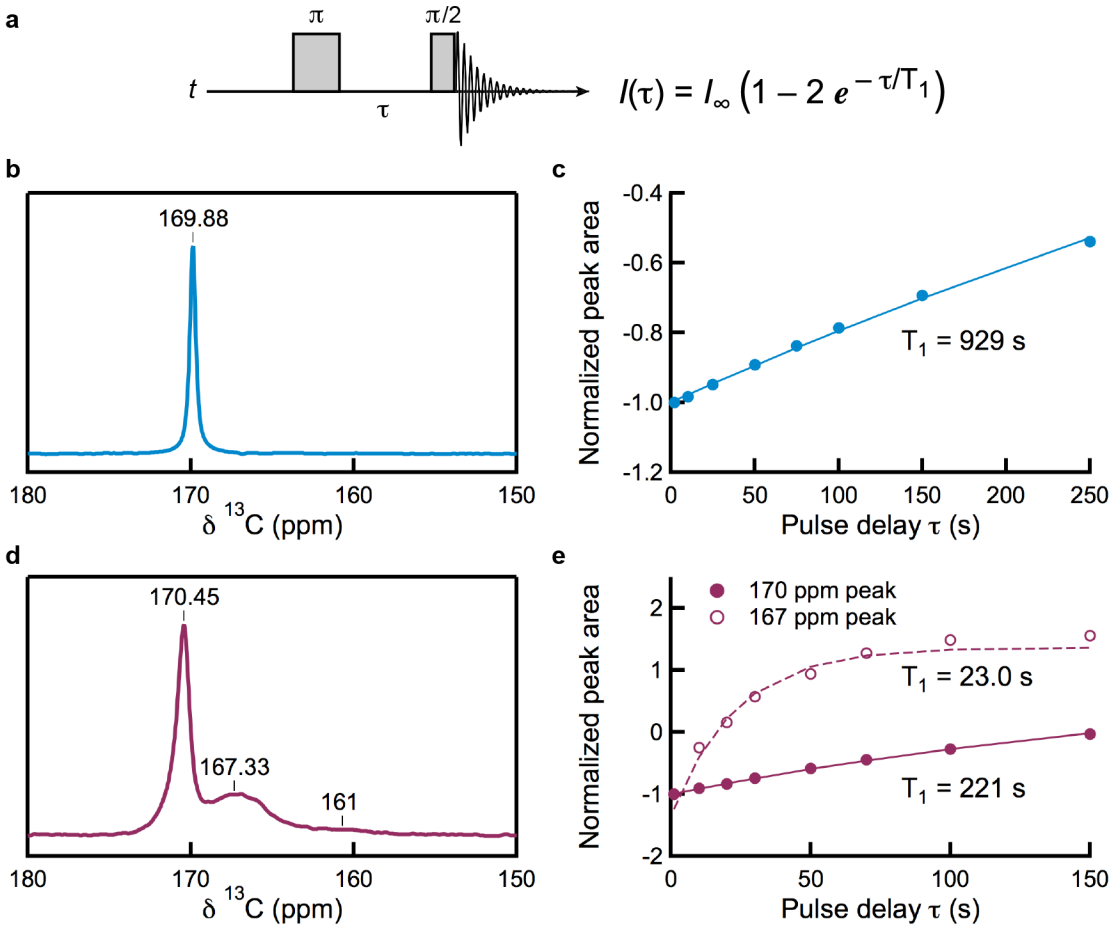

Supplementary Figure 5 | Magnetic relaxation measurements of bulk $K_2{}^{13}CO_3$ and $K_2{}^{13}CO_3/TiO_2$ (2x). **a**, Schematic representation of the inversion recovery pulse sequence and fit function used to quantify longitudinal relaxation (T_1). **b**, ^{13}C NMR spectrum and **c**, inversion recovery fit of bulk $K_2{}^{13}CO_3$, showing that the bulk crystalline solid displays a single resonance with very slow relaxation dynamics. **d**, ^{13}C NMR spectrum of $K_2{}^{13}CO_3/TiO_2$ (2x), showing line broadening and the presence of an additional resonance relative to the bulk crystalline species, which we assign to surface-bound CO_3^{2-}. The weak shoulder at $\delta_{iso} \sim 161$ ppm is assigned to residual HCO_3^- resulting from the aqueous sample preparation. **e**, Inversion recovery fit for the two major resonances of $K_2{}^{13}CO_3/TiO_2$ (2x), showing dramatically reduced T_1 values. All spectra were collected with 5 kHz magic angle spinning in a standard 5 mm rotor.

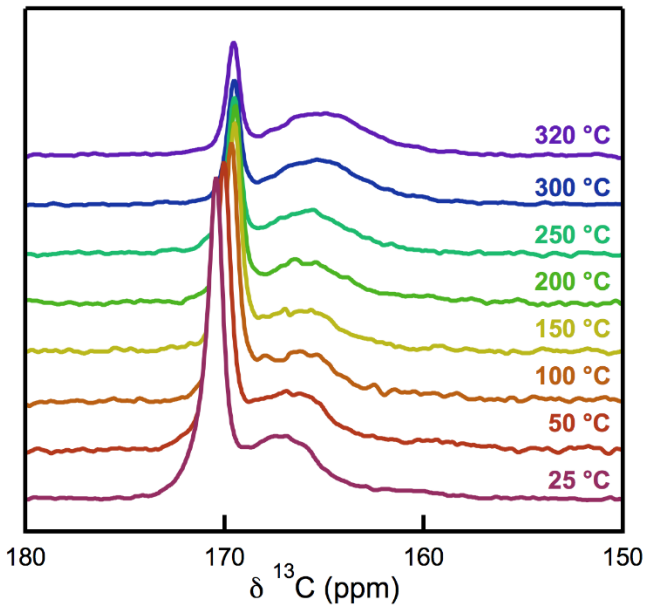

Supplementary Figure 6 | ^{13}C Magic Angle Spinning (MAS) NMR spectra of $K_2{}^{13}CO_3/TiO_2$ (2x) collected at elevated temperatures using sealed "WHiMS" rotors.

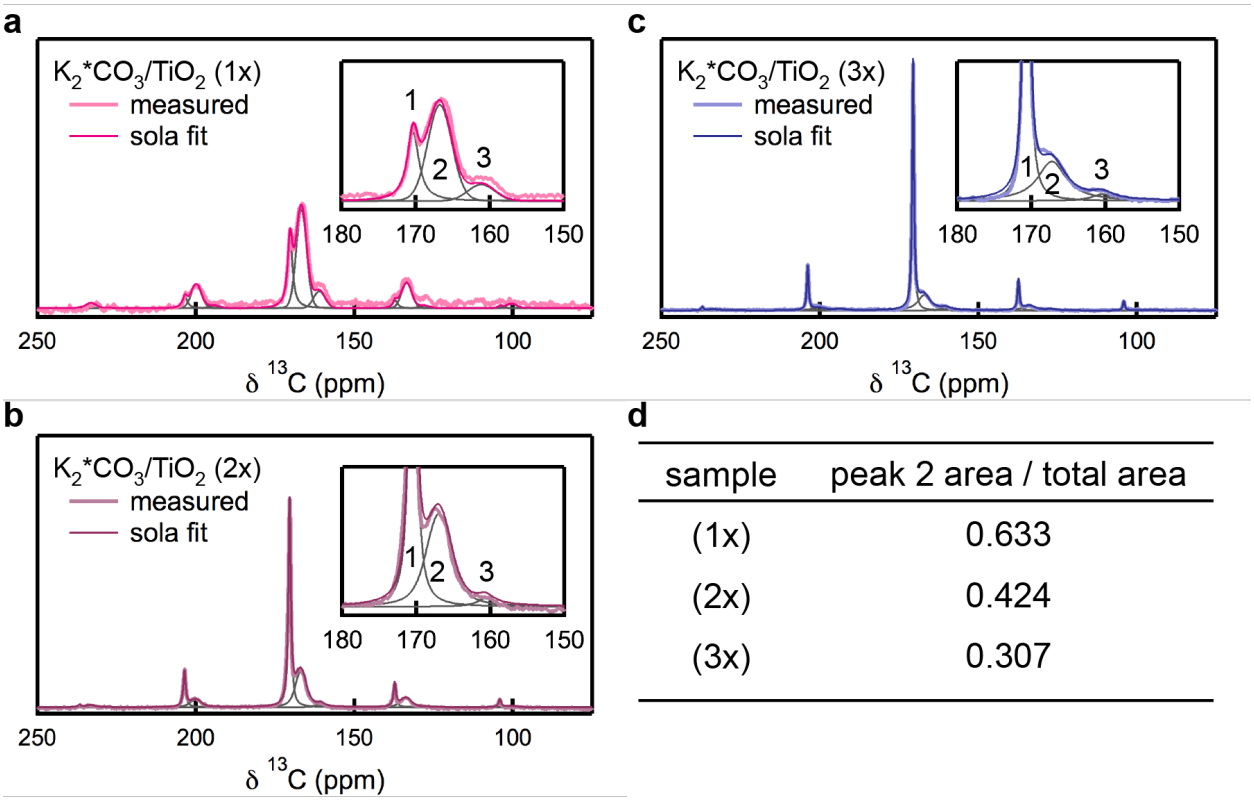

d

sample	peak 2 area / total area
(1x)	0.633
(2x)	0.424
(3x)	0.307

Supplementary Figure 7 | Solid state NMR quantification of ^{13}C speciation in $K_2{}^{13}CO_3/TiO_2$ (1–3x). **a–c**, Room temperature ^{13}C direct polarization spectra of $K_2{}^{13}CO_3/TiO_2$ (1–3x), overlaid with spectra simulated using the "sola" solid state peak fitting program. The region containing the isotropic resonances of carbonate species is shown in the insets. Experimental spectra were measured in a 5 mm rotor with 5 kHz magic angle spinning (MAS). No ^{1}H decoupling field was applied, and a sufficient recycle delay was used between pulses to allow for > 95% recovery of longitudinal magnetization for all resonances based on T_1 quantification. Simulated spectra were modeled using three sites at δ_{iso} ~ 170, 167, and 161 ppm, corresponding to crystalline $^{13}CO_3^{2-}$, surface-bound $^{13}CO_3^{2-}$, and $H^{13}CO_3^-$, respectively. Simulated spectra were fit to experimental ^{13}C spectra by refining the parameter for MAS rate as well as the δ_{iso}, intensity, line broadening, δ_{CSA}, and η_{CSA} parameters for each site until at least 75% overlap between the simulated and experimental spectrum was achieved. **d**, Table showing fraction of surface-bound $^{13}CO_3^{2-}$ present in $K_2{}^{13}CO_3/TiO_2$ (1–3x), as determined by integral ratio of peaks from the simulated spectra.

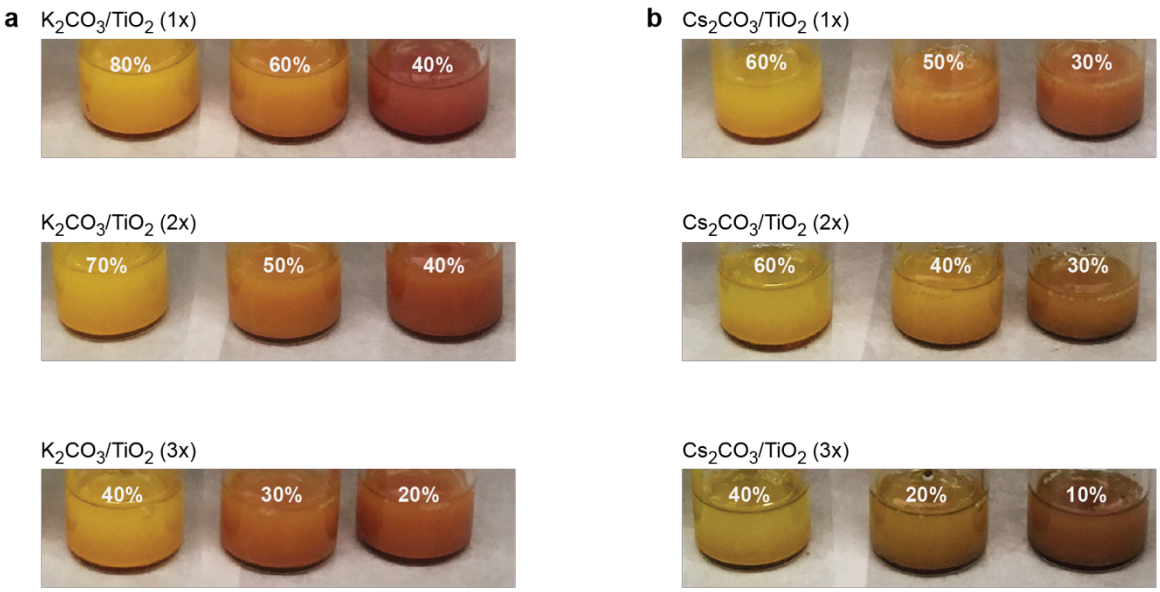

Supplementary Figure 8 | Titration studies of **a**, K_2CO_3/TiO_2 (1–3x) and **b**, Cs_2CO_3/TiO_2 (1–3x). In an inert atmosphere glovebox, various quantities of 4-nitrophenol (0.2 wt% in benzene, pK_a = 7.2 in H_2O) were added to M_2CO_3/TiO_2 (50 mg in 2 mL benzene), causing the sample to turn yellow as surface carbonates deprotonate the phenolic proton. The amount of 4-nitrophenol added to each sample (% relative to M_2CO_3) is labeled in white. The sample was equilibrated for ~15 minutes with gentle shaking, after which phenolphthalein (saturated solution in benzene, 2 mL) was added. If the amount of 4-nitrophenol was not enough to quench all the surface carbonates, the sample darkened and gained a red/violet tint due to the presence of deprotonated phenolphthalein. Based on these titration results, approximately 60, 50, and 30% of the carbonates are exposed in K_2CO_3/TiO_2 (1x), (2x), and (3x), respectively; and approximately 50, 40, and 20% are exposed in Cs_2CO_3/TiO_2 (1x), (2x), and (3x), respectively.

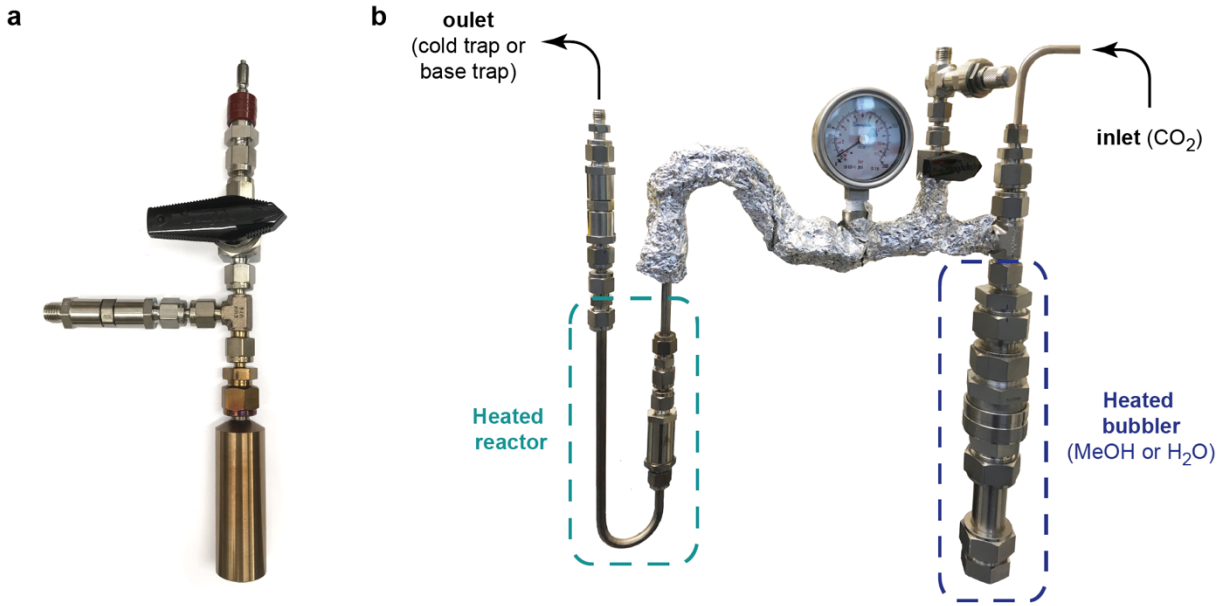

Supplementary Figure 9 | **a**, Stainless steel miniature batch reactor (27.5 mL) used for carboxylation reactions. The reactor is equipped with a valve and quick-connect fitting for gas dosing, as well as a safety check valve. The reactor is heated using insulated heat tape. **b**, Stainless steel flow reactor setup used for volatilization reactions. A stainless steel bubbler containing either methanol or H_2O is heated using insulated heat tape (typically, 70–80 °C for MeOH and 110 °C for H_2O) to achieve the desired vapor partial pressures. A second heat tape is wrapped around the reactor, and set to a different temperature (typically, 250–280 °C for MeOH volatilizations, and 380 °C for H_2O). The total pressure is set by a downstream check valve and monitored using the pressure gauge.

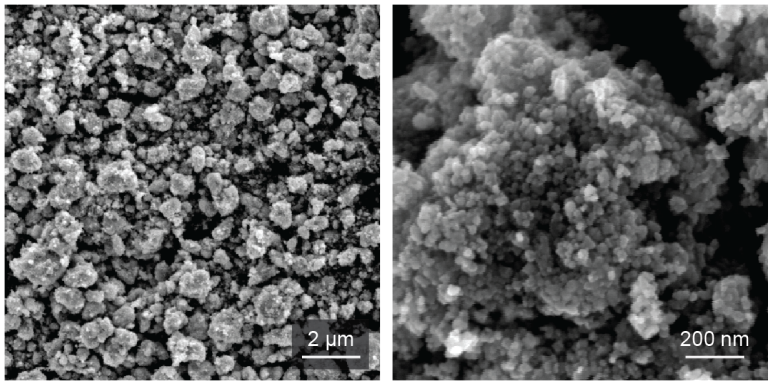

Supplementary Figure 10 | SEM images of commercial TiO_2 pellets that have been ground up by mortar and pestle, with a BET surface area of 38.1(4) m^2/g, pore volume of 0.17 cm^3/g, and a broad pore distribution centered at 11 nm.

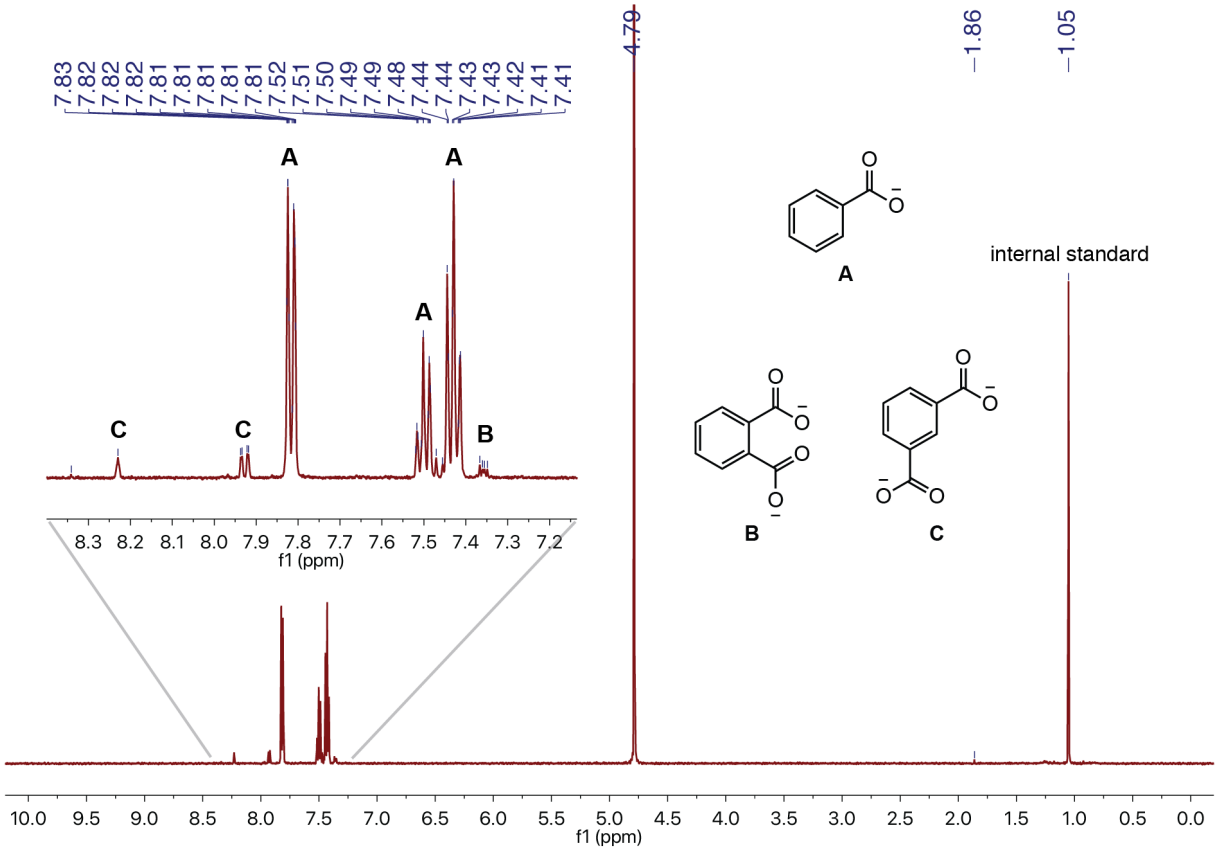

Supplementary Figure 11 | ^{1}H NMR (500MHz) in D_2O of the extracted product mixture after a benzene carboxylation reaction with Cs_2CO_3/TiO_2 (1x) under 20 bar benzene and 10 bar CO_2 at 420 °C for 3 h. Mono- and small amounts of di-carboxylates are formed in the reaction. Sodium pivalate was used as the internal standard.

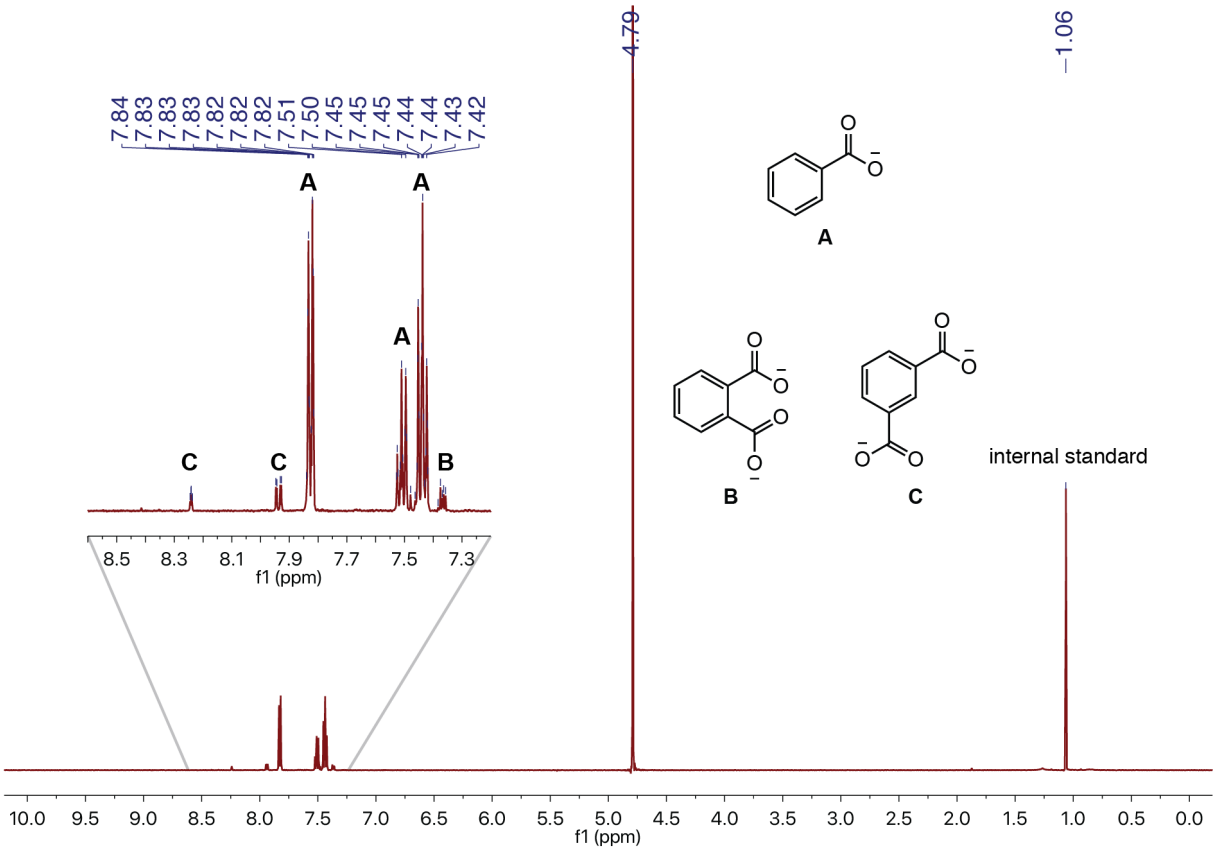

Supplementary Figure 12 | ^{1}H NMR (500MHz) in D_2O of the extracted product mixture after a benzene carboxylation reaction with K_2CO_3/TiO_2 (1x) under 20 bar benzene and 10 bar CO_2 at 440 °C for 3 h. Mono- and small amounts of di-carboxylates are formed in the reaction. Sodium pivalate was used as the internal standard.

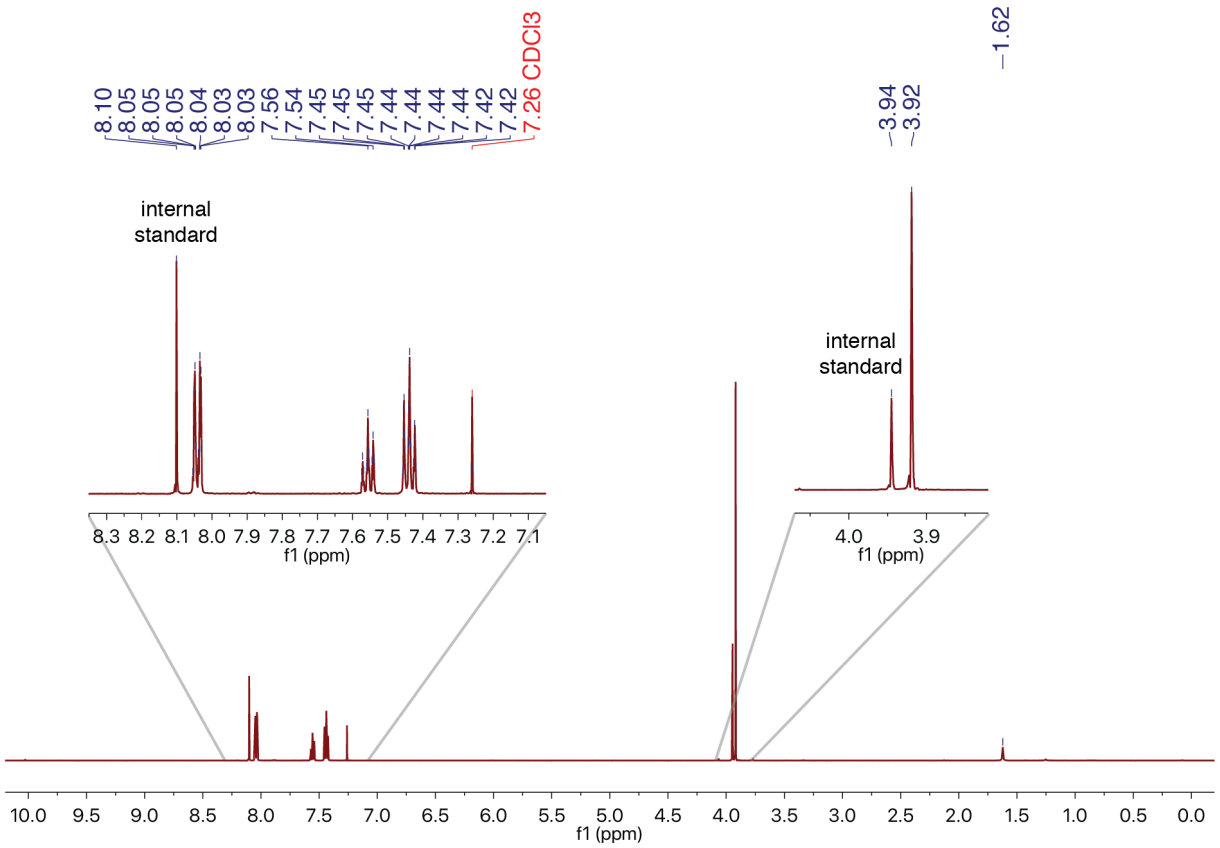

Supplementary Figure 13 | ^{1}H NMR (500MHz) in $CDCl_3$ of volatilized methyl benzoate, obtained from methylation of cesium benzoate on Cs_2CO_3/TiO_2 (1x). Methylation conditions: 1.8 bar MeOH, 1.2 bar CO_2, flowing 100 ml/min at 250 °C for 1 h. Dimethyl terephthalate was used as the internal standard.

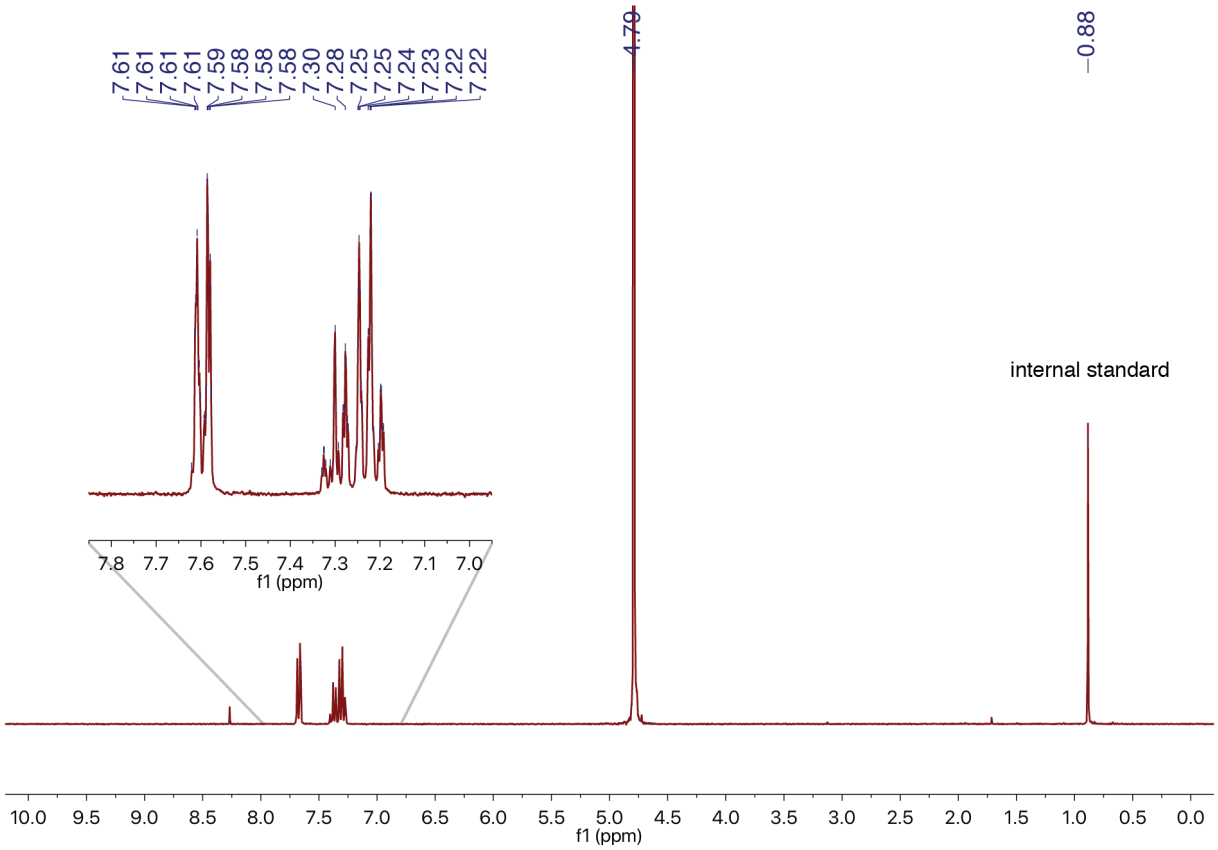

Supplementary Figure 14 | ^{1}H NMR (300MHz) in D_2O of benzoate, obtained from hydrolysis of the volatilized methyl benzoate produced on Cs_2CO_3/TiO_2 (1x). Carboxylation conditions: 20 bar benzene and 10 bar CO_2, 440 °C for 0.5 h. Methylation conditions: 1.8 bar MeOH, 1.2 bar CO_2, flowing 100 ml/min at 250 °C for 1 h. Note: trace formate (~8.3 ppm) was produced from methanol decomposition during the hydrolysis workup and not from the methylation reaction. Sodium pivalate was used as the internal standard.

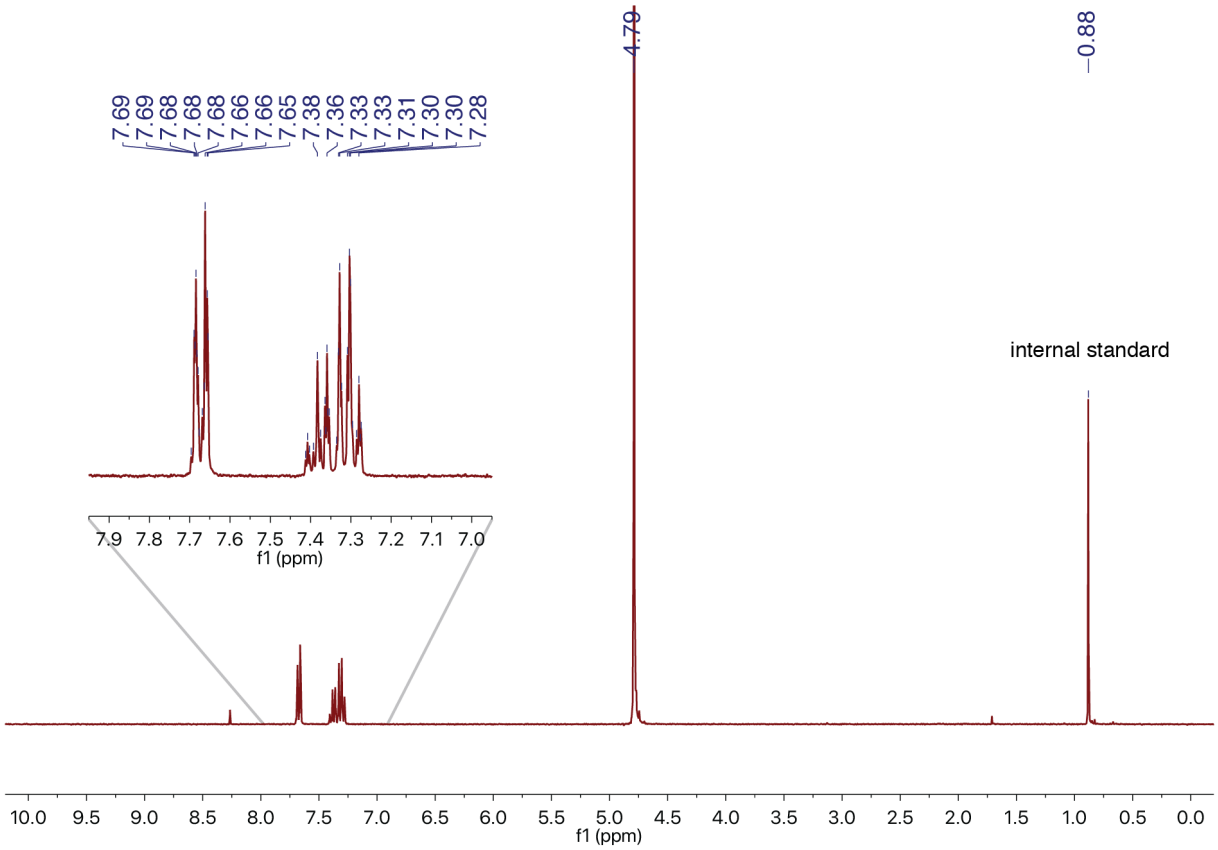

Supplementary Figure 15 | ^{1}H NMR (300MHz) in D_2O of benzoate, obtained from hydrolysis of the volatilized methyl benzoate produced on K_2CO_3/TiO_2 (1x). Carboxylation conditions: 20 bar benzene and 10 bar CO_2, 440 °C for 3 h. Methylation conditions: 1.8 bar MeOH, 1.2 bar CO_2, flowing 100 ml/min at 280 °C for 1 h. Note: trace formate (~8.3 ppm) was produced from methanol decomposition during the hydrolysis workup and not from the methylation reaction. Sodium pivalate was used as the internal standard.

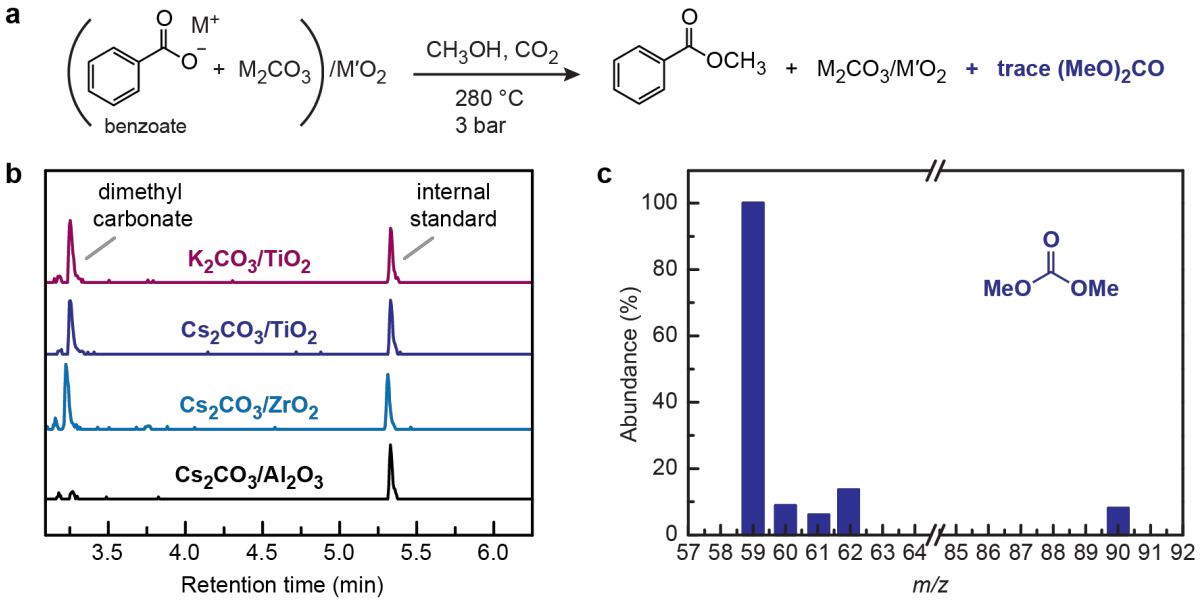

Supplementary Figure 16 | **a**, Surface-bound benzoate species were volatilized as methyl benzoate under flowing MeOH/CO_2 conditions (280 °C, 3 bar, 100 mL/min for 2 h) and trapped in a downstream cold trap. Trace dimethyl carbonate was observed in the cold trap by GC-MS along with the product methyl benzoate. **b**, GC-MS data of the cold trap following benzoate methylation on K_2CO_3/TiO_2, Cs_2CO_3/TiO_2, Cs_2CO_3/ZrO_2, and $Cs_2CO_3/\gamma\text{-}Al_2O_3$. Toluene was used as the internal standard. **c**, Mass spectrum of dimethyl carbonate.

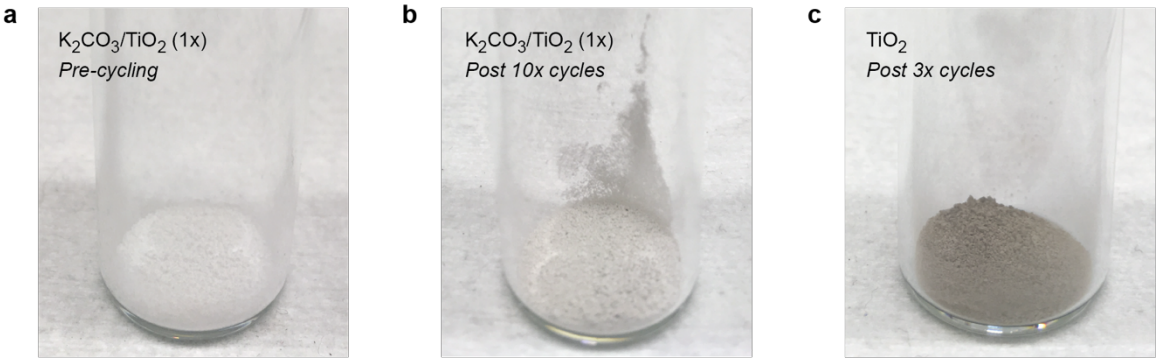

Supplementary Figure 17 | Images of **a**, K_2CO_3/TiO_2 (1x) before cycling; **b**, K_2CO_3/TiO_2 (1x) after 10x benzene carboxylation cycles; and **c**, bare TiO_2 support after 3x benzene carboxylation cycles.

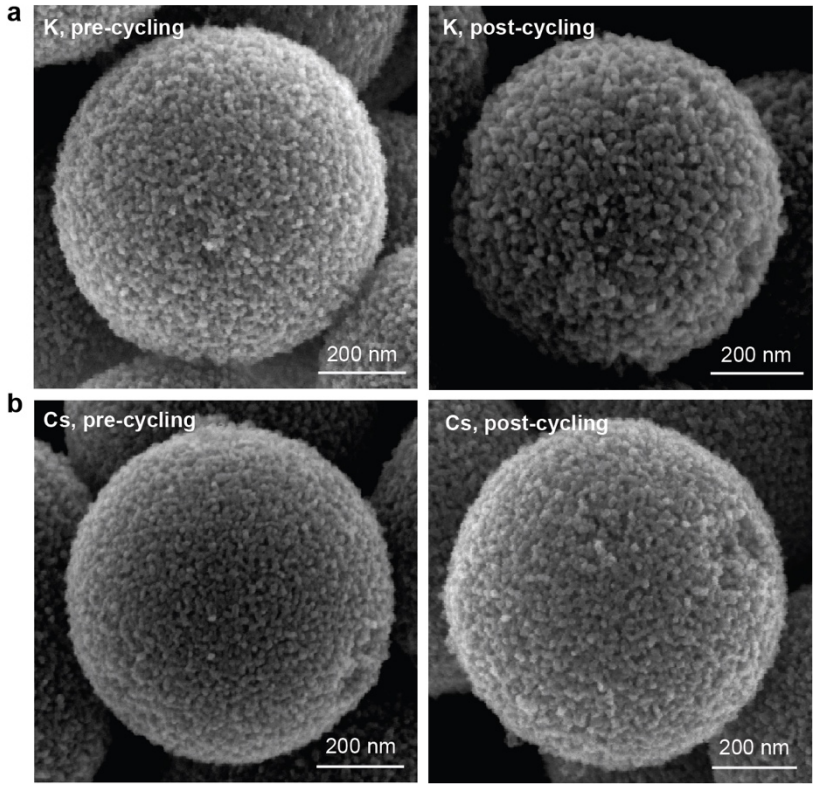

Supplementary Figure 18 | SEM images of **a**, K_2CO_3/TiO_2 (1x) and **b**, Cs_2CO_3/TiO_2 (1x) before and after 10x benzene CO_2 insertion cycling experiments. Greater sintering/grain coarsening of the TiO_2 nanocrystallites was observed in K_2CO_3 relative to Cs_2CO_3/TiO_2 (1x) because the carboxylation reactions were performed for significantly longer times (3 h at 440 °C versus 0.5 h at 440 °C).

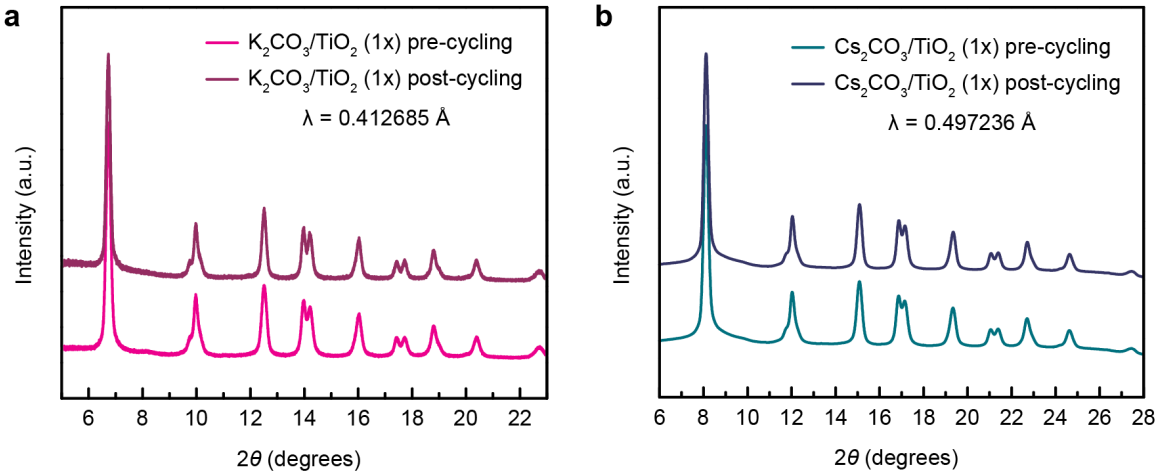

Supplementary Figure 19 | pXRD patterns of **a**, K_2CO_3/TiO_2 (1x) (λ = 0.412685 Å) and **b**, Cs_2CO_3/TiO_2 (1x) (λ = 0.497236 Å) before and after 10x benzene CO_2 insertion cycling experiments.

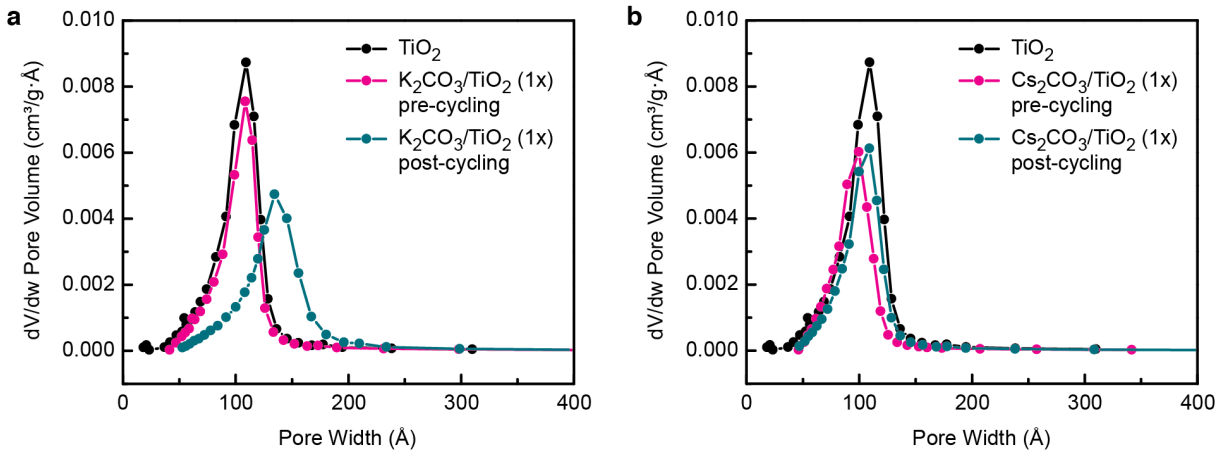

Supplementary Figure 20 | Pore size distribution plots of **a**, K_2CO_3/TiO_2 (1x) and **b**, Cs_2CO_3/TiO_2 (1x) before and after 10x benzene CO_2 insertion cycling experiments, calculated using the Barrett–Joyner–Halenda (BJH) method from 77 K N_2 isotherm data (desorption branch). Greater sintering/grain coarsening of the TiO_2 nanocrystallites, which led to a change in the pore size distribution plot, was observed in K_2CO_3 relative to Cs_2CO_3/TiO_2 (1x) because the carboxylation reactions were performed for significantly longer times (3 h at 440 °C versus 0.5 h at 440 °C).

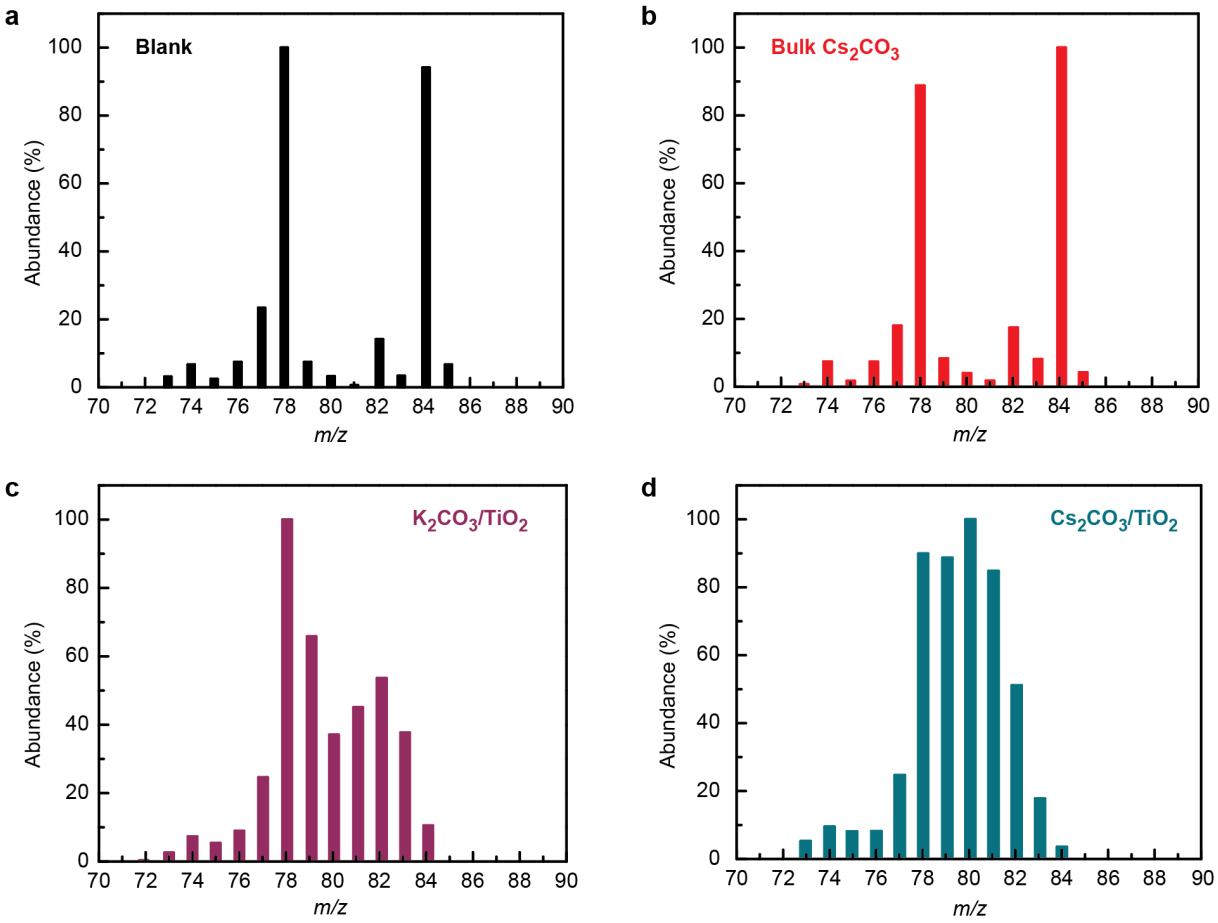

Supplementary Figure 21 | Mass spectra showing the results of H/D exchange experiments performed using M_2CO_3/TiO_2 (1x) (333 mg) and a 1:1 mixture of C_6H_6:C_6D_6 (20 µl). **a**, Control experiment with a bare reactor under N_2; **b**, control experiment using bulk Cs_2CO_3 (500 mg) under N_2; **c**, K_2CO_3/TiO_2 (1x) under N_2; and **d**, Cs_2CO_3/TiO_2 (1x) under N_2.

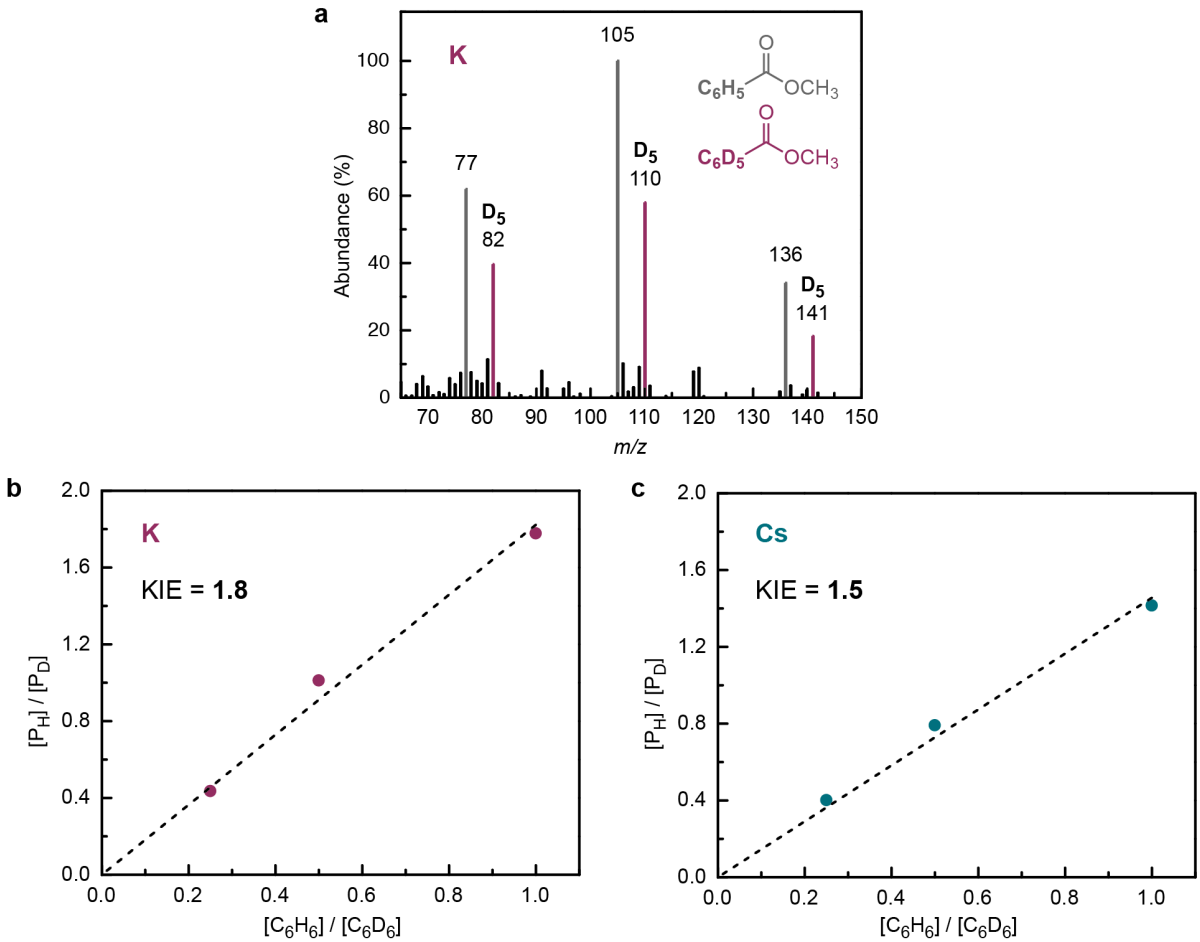

Supplementary Figure 22 | Determination of kinetic isotope effect (KIE) values for the carboxylation of benzene by K_2CO_3 and Cs_2CO_3/TiO_2 (1x). **a**, Mass spectrum of a mixture of methyl benzoate-d_0 and d_5 derived from a K_2CO_3/TiO_2 (1x) carboxylation reaction using a 1:1 mixture of C_6H_6 and C_6D_6. **b**, The ratio of protio to deuterated products, $[P_H]/[P_D]$, was plotted versus the initial $[C_6H_6]/[C_6D_6]$ ratio. The slope obtained from fitting these points to a line is the KIE, which was determined to be 1.8 and 1.5 for K_2CO_3 and Cs_2CO_3/TiO_2 (1x), respectively.

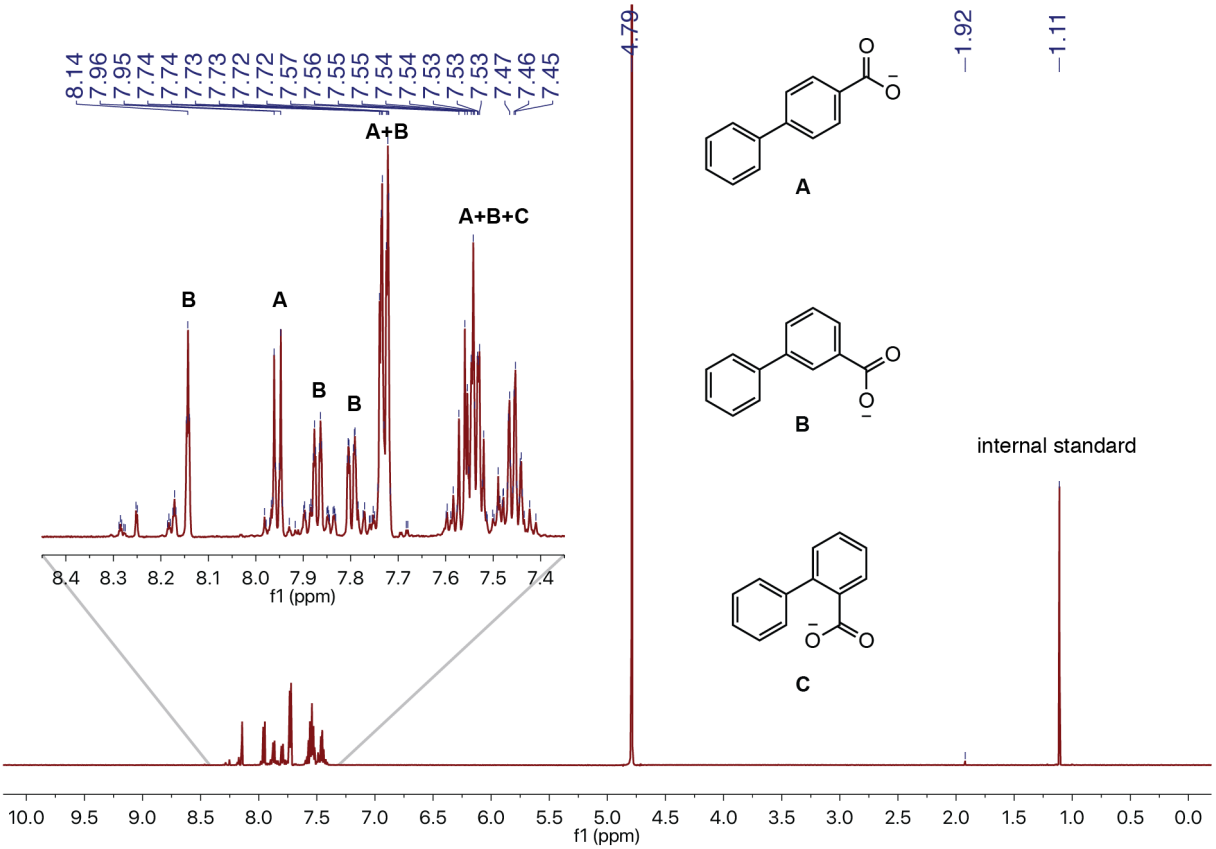

Supplementary Figure 23 | ^{1}H NMR (600MHz) in D_2O of the extracted product mixture after a biphenyl carboxylation reaction with Cs_2CO_3/TiO_2 (1x) under 600 mg biphenyl (7.5 bar) and 10 bar CO_2 at 420 °C for 3 h. Mono- and small amounts of dicarboxylates are formed in the reaction. Sodium pivalate was used as the internal standard. Due to the complicated aromatic region, only cesium 3- and 4-biphenylcarboxylate could be quantified from ^{1}H NMR; other carboxylate salts were quantified by HPLC.

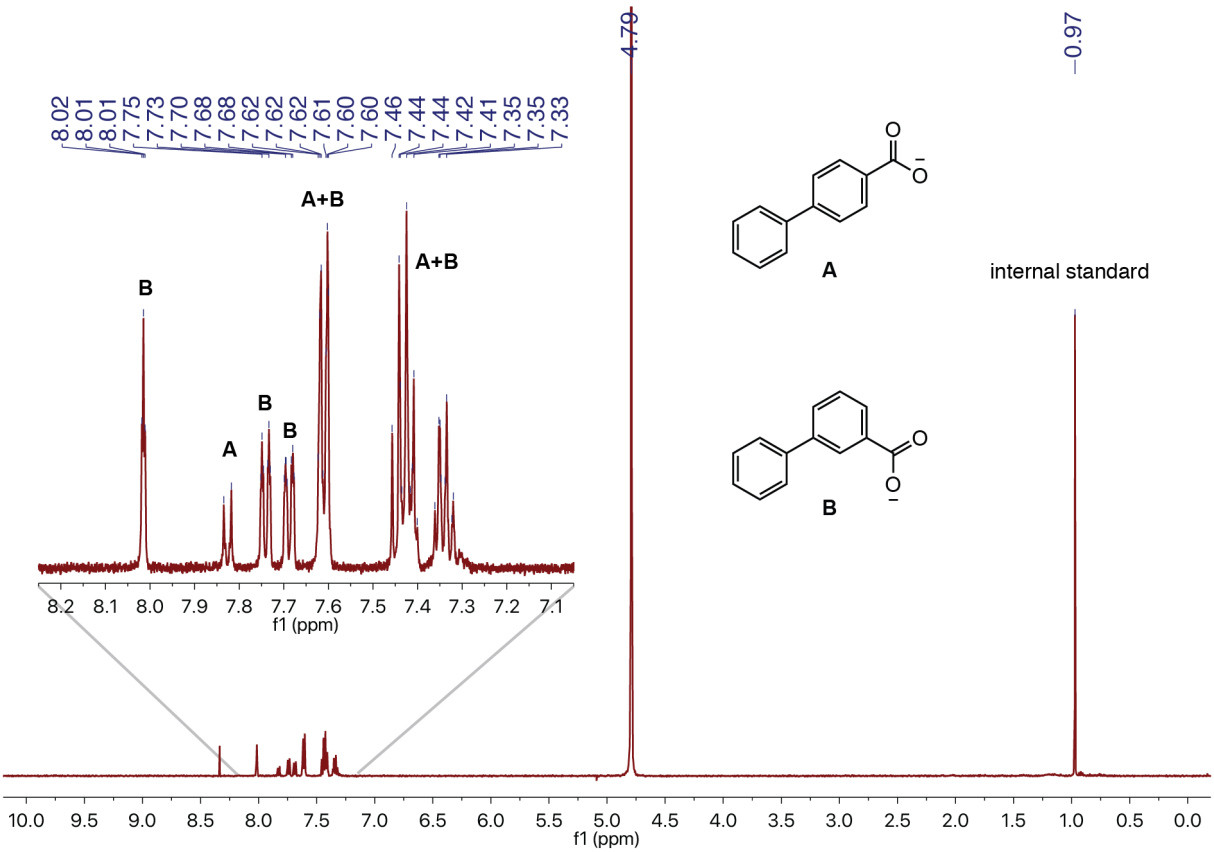

Supplementary Figure 24 | ^{1}H NMR (500MHz) in D_2O of 3- and 4-biphenylcarboxylate, obtained from hydrolysis of the volatilized methyl esters produced on Cs_2CO_3/TiO_2 (1x). Carboxylation conditions: 600 mg biphenyl (7.5 bar) and 10 bar CO_2, 420 °C for 3 h. Methylation conditions: 1.8 bar MeOH, 1.2 bar CO_2, flowing 100 ml/min at 280 °C for 2 h. Note: formate (~8.3 ppm) was produced from methanol decomposition during the hydrolysis workup and not from the methylation reaction. Sodium pivalate was used as the internal standard.

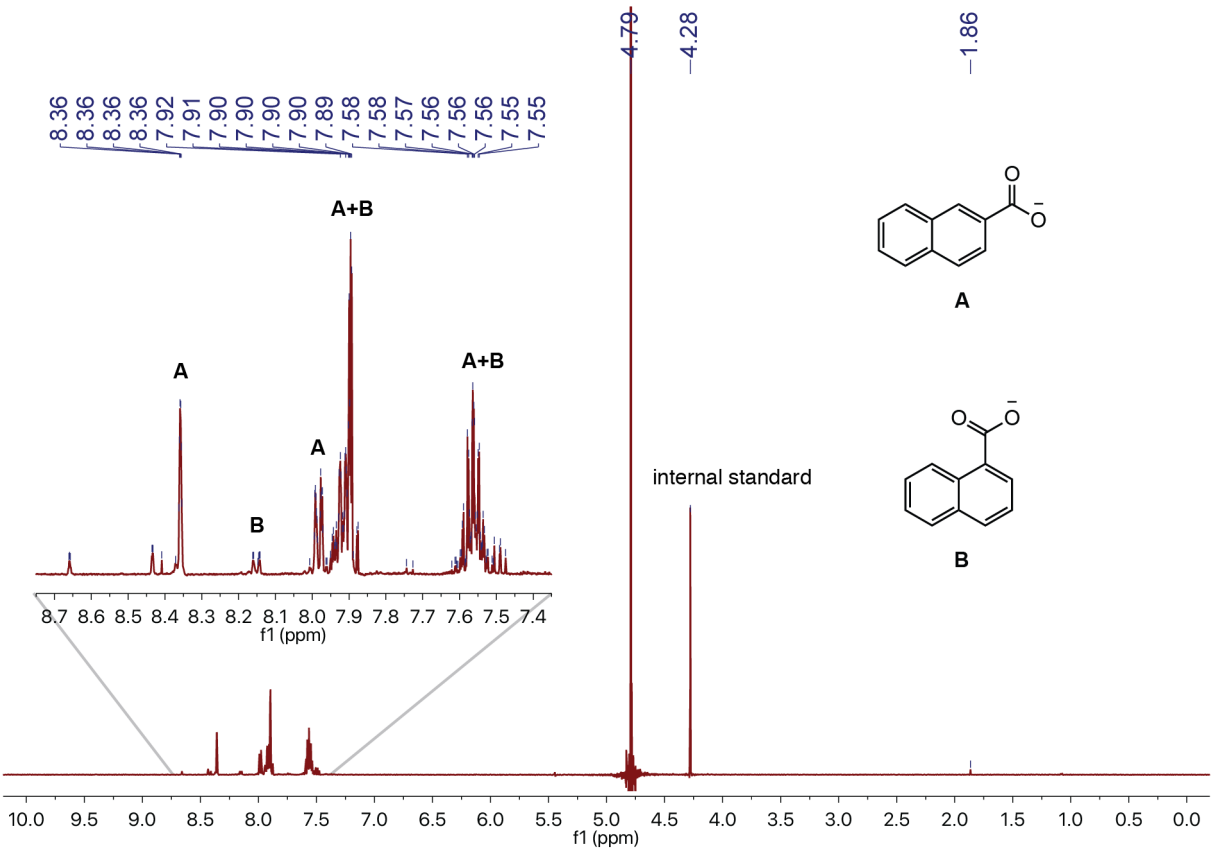

Supplementary Figure 25 | ^{1}H NMR (500MHz) in D_2O of the extracted product mixture after a naphthalene carboxylation reaction with Cs_2CO_3/TiO_2 (1x) under 250 mg napthalene (3.8 bar) and 10 bar CO_2 at 400 °C for 3 h. Mono- and small amounts of dicarboxylates are formed in the reaction. Sodium tartrate was used as the internal standard. Due to the complicated aromatic region, quantification of carboxylate salts were performed using a combination of ^{1}H NMR and HPLC.

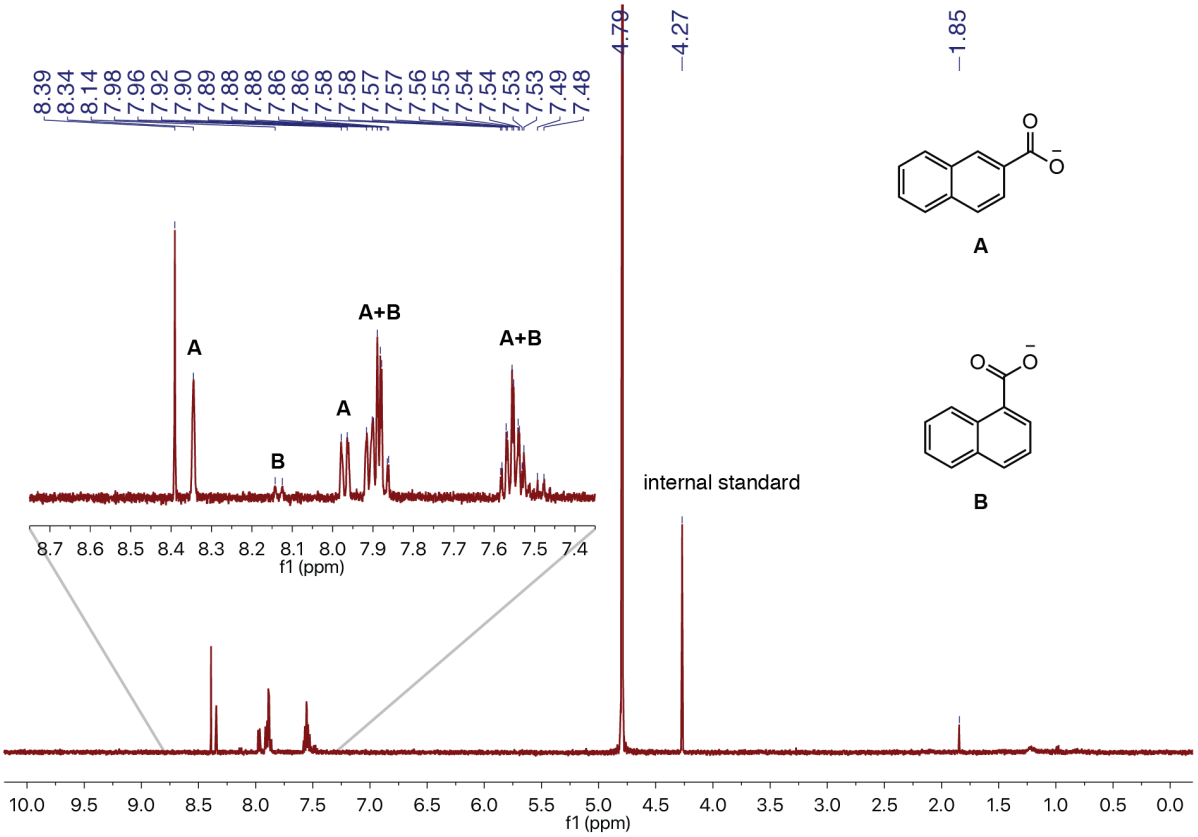

Supplementary Figure 26 | ^{1}H NMR (500MHz) in D_2O of 1- and 2-naphthoate, obtained from hydrolysis of the volatilized methyl esters produced on Cs_2CO_3/TiO_2 (1x). Carboxylation conditions: 250 mg naphthalene (3.8 bar) and 10 bar CO_2, 400 °C for 3 h. Methylation conditions: 1.8 bar MeOH, 1.2 bar CO_2, flowing 100 ml/min at 280 °C for 2 h. Note: formate (~8.4 ppm) was produced from methanol decomposition during the hydrolysis workup and not from the methylation reaction. Sodium tartrate was used as the internal standard.

4. References

1. Jun, S. *et al.* Synthesis of New, Nanoporous Carbon with Hexagonally Ordered Mesostructure. *J. Am. Chem. Soc.* **122**, 10712–10713 (2000).
2. Walter, E. D. *et al. Operando* MAS NMR Reaction Studies at High Temperatures and Pressures. *J. Phys. Chem. C* **122**, 8209–8215 (2018).
3. Mehta, H. S. *et al.* A novel high-temperature MAS probe with optimized temperature gradient across sample rotor for in-situ monitoring of high-temperature high-pressure chemical reactions. *Solid State Nucl. Magn. Reson.* S092620401930058X (2019). doi:10.1016/j.ssnmr.2019.06.003
4. Bielecki, A. & Burum, D. P. Temperature Dependence of 207 Pb MAS Spectra of Solid Lead Nitrate. An Accurate, Sensitive Thermometer for Variable-Temperature MAS. *J. Magn. Reson. A* **116**, 215–220 (1995).
5. Ono, Y. & Hattori, H. Characterization of Solid Base Catalysts. in *Solid Base Catalysis* **101**, 11–68 (Springer Berlin Heidelberg, 2011).
6. Tanabe, K. & Yamaguchi, T. BASICITY AND ACIDITY OF SOLID SURFACES. *J. Res. Inst. Catal. HOKKAIDO Univ.* **11**, 179–184 (1964).